© 2018

MEHMET AKIF GORMEZ

ALL RIGHTS RESERVED

DRIVING CYCLE OPTIMIZATION OF AN ELECTRIC CITY BUS NETWORK

A Thesis Presented to

The Graduate School of The University of Akron

In Partial Fulfillment

of the Requirements for Degree

Master of Science

Mehmet Akif Gormez

August 2018

DRIVING CYCLE OPTIMIZATION OF AN ELECTRICCITY BUS NETWORK

Mehmet Akif Gormez

Thesis

Approved:

_____
Advisor
Dr. Yilmaz Sozer

_____
Committee Member
Dr. J. Alexis De Abreu Garcia

_____
Committee Member
Dr. Malik Elbuluk

Accepted:

_____
Interim Department Chair
Dr. Robert J. Veillette

_____
Dean of the College
Dr. Donald P. Visco

_____
Dean of the Graduate School
Dr. Chand Midha

_____
Date

ABSTRACT

Hazardous impact of fossil fuel usage in transportation is forcing industry to improve environmentally-friendly transportation solutions. In this thesis, ‘opportunity charging’ (which means to charge the vehicle on every opportunity) city bus networks have been investigated. An electric vehicle model has been developed and simulated for energy consumption; a driving cycle optimization algorithm is developed to reduce the energy consumption by the EV and to use optimal charging time on each stop considering its impact on battery lifetime in respect to the bus schedule. The results are demonstrated in case studies. Proposed charging pattern (the opportunity charging) and the optimized driving cycle indicate that the overall cost of an electric bus network can be reduced significantly.

ACKNOWLEDGMENTS

I would like to share my deep, sincere gratitude with my adviser, Dr. Yilmaz Sozer, for his sincere advice, guidance, and support during my study at The University of Akron. His technical skills have been a source of creativity and encouragement for me and will remain so during my future career, my committee members, Dr. J. Alexis De Abreu-Garcia and Dr. Malik Elbuluk, for their expertise and support that shapes my future career in academia, my colleagues, whose example and friendship will remain to guide me to become the best student, friend, and researcher, and my family members and friends for their support, and motivation which I would not be here writing this thesis without.

TABLE OF CONTENTS

Page:

LIST OF TABLES……viii

LIST OF FIGURES……ix

CHAPTER:

I. INTRODUCTION 1

1.1. Electric Vehicles 1

1.2. Thesis Objectives 5

II. LITERATURE REVIEW 7

2.1. Vehicle Model 7

2.2. Vehicle Powertrain Technology 11

2.2.1. Parallel Powertrain Architecture 11

2.2.2. Series Architecture 12

2.2.3. Electric Machine Selection 14

2.3. Battery Storage 16

2.4. Charging Patterns for Electric Bus Networks 19

2.5. Optimization Methods 22

2.3.1. Linear Programming 22

2.3.2. Dynamic Programming 23
2.3.3. Genetic Algorithms 23
2.3.4. Particle Swarm Optimization 24
2.3.5. Driving Cycle Optimization 25
2.6. Conclusions 27
III. SYSTEM PRESENTATION AND SIMULATION 28
3.1. Electric Machine Drive System 28
3.2. Vehicle Model 31
3.2.1 Vehicle Powertrain 32
3.2.2 Vehicle Mechanics 34
3.2.3 Route Conditions 37
3.3. Battery Degradation Model 40
3.4. Driver Model 42
3.5. Simulation of the EV Bus 43
3.6. Simulation Results 44
3.7. Conclusions 45
IV. OPTIMIZATION 47
4.1. Problem Formulation 47
4.2. PSO Algorithm 50
4.3. Optimization Process 53
4.4. Conclusions 54
V. Case Optimization and Simulation Results 56

5.1. Case Studies 56
5.1.1 Case Study I 57
5.1.2 Case Study II 59
5.1.3 Case Study III 62
5.2. Reduction of Battery Capacity 64
5.3. Conclusions 65
VI. CONCLUSION 66
REFERENCES: 70
APPENDIX A: Electric Vehicle Simulation 74
APPENDIX B: Source Code 75

LIST OF TABLES

Table: Page:

2.1: Comparison of conventional and electrical powertrain. 11

2.2: Evaluation of the electric machine types. 16

2.3: Properties of EV batteries 17

3.1: Powertrain sizing of the vehicle 33

3.2: Coefficients used for the vehicle model. 37

5.1: Optimization results for case 1.. 59

5.2: Optimization results for case 2. 61

5.3: Optimization results for case 3. 64

5.4: Required minimum battery capacity for case studies. 65

LIST OF FIGURES

Figure: Page:

1.1: EV system components. 2

1.2: a) Annual operating cost of different types of electric bus. b) Cost of acquiring different type electric buses. 3

1.3: Proposed bus network topology and its optimization. 4

2.1: : Free body diagram of a vehicle.. 8

2.2: Energy consumption results of test and simulation for different routes considered. .10

2.3: Parallel vehicle architecture. 12

2.4: Series architecture 12

2.5: Possible powertrain designs for EV bus application. a) Four-wheel drive with four motors. b) Four-wheel drive with four motors with the differential on the front. c) Rear wheel drive only. d) Four-wheel drive with one motor. 14

2.6: Efficiency maps of different machines. 16

2.7: Charging schemes for electric bus networks. 20

2.8: Overnight charging topology with battery SOC levels. a) Overnight charging. b) Opportunity charging 21

2.9: Driving cycle optimization methods 22

2.10: Shortest path between point B to H or vise-versa. 23

2.11: Stages of GA 24

2.12: Particles and their velocities in PSO. 25

3.1: a) Block diagram of electric vehicle drive system. b) A visual of electric vehicle drive system. 29

3.2: Motor drive system test set-up. 30

3.3: Efficiency map of the motor drive system. a) Tested operation points and their efficiency. b) Interpolated efficiency map. 31

3.4: Description of the powertrain considered in the study. 33

3.5: Rolling resistance force occurred on a wheel. 35

3.6: Role of the route conditions in EV energy consumption 39

3.7: Route conditions block. 40

3.8: Driver model used to drive the vehicle. 43

3.9: Electric vehicle model used to determine its energy demand (energy consumption) and battery cost. 44

3.10: Simulation result for different road grades. a) Road grade = 0 . b) Road grade = 5. c) Road grade = 10 45

4.1: Implemented penalty function. 49

4.2: System costs and their contribution to the global cost. 49

4.3: Developed PSO for driving cycle optimization 51

4.4: The global cost and the leaders of an interval as the iteration number increases. a) Leader particles b) Global cost. 53

4.5: Block diagram of the optimization process. 54

5.1: Route conditions of the case study 1. a) Road grade. b) Speed limit. 57

5.2: Visual representation of the bus route. 57

5.3: Optimized results for the first case study. a) Speed profile and time spent (driving and charging) on each interval of the route. b) Optimized battery SOC and cost 58
5.4: Route conditions for case study. a) Speed limit. b) Road slope. c) Wind speed d) Passenger quantity. 60
5.5: EV bus and its considered route condition for the case study. 60
5.6: Optimized results for the second case study. a) Speed profile and time spent (driving and charging) on each interval of the route. b) Optimized battery SOC and cost 61
5.7: Route conditions for case study. a) Road slope. b) Wind Speed. c) Speed limit. 62
5.8: A visual representation of the bus route 63
5.9 Optimized results for the third case study. a) Speed profile and time spent (driving and charging) on each interval of the route. b) Optimized battery SOC and cost. 63
5.10: Considered bus route using previous case studies. 64

CHAPTER I

INTRODUCTION

1.1. Electric Vehicles

The recent development of Electric Vehicles (EV) has been immediate and accelerating due to the increasing fossil fuel usage in industry and its harmful effects on the environment. An EV is a vehicle that uses electric motors as an impulsive power source instead of an internal combustion engine (ICE); as a result, it does not directly produce greenhouse gases. Furthermore, the fuel efficiency (mile per currency) of electric vehicles is considerably higher than that of non-EVs, which makes them good candidates for a prime means of medium and short-range transportation. Moreover, the market share of EVs is also expected to explode in the near future. According to a research survey [1], a significant number of drivers are highly interested in buying an EV as their daily transportation vehicle. Even though a considerable market penetration is expected, EV technologies still suffer from low driving ranges and high battery costs.

Lack of maturity in technologies like electro-mechanics, computer technology, and electrical energy storage has led to a century of delay in market capitalization of EV products. EV history goes back to the 1800s. Although modern studies start in 1916, when the first hybrid/electric vehicle was invented, and many of the limitations on EV products have been overcome by engineers; however, the short driving range and long charging time of the technology is still below market expectations today [2]. Accordingly, many

researchers have focused their attention on efficient energy management and eco-driving techniques to increase the driving range while reducing the need for charging [3-4].

Though EVs may not be a prime choice for long-range travelers, they might be convenient transportation means for inner-city trips because of their cheaper maintenance and operating costs. A typical electric bus might have components like electric machine, energy storage systems, power electronics, power receivers, and controls. The electric machine (or machines, there might be multiple) receives its energy from the energy storage unit like batteries, and the batteries are charged via either the power receiver units or the electric machine. The power electronics are used to conduct the power flow between the electric machine, the power receiver unit, and the storage systems. The controls unit makes the power flow control possible between the vehicle's components. A typical electric bus and its components are described in Fig. 1.1. Thus, the electric buses do not use conventional costly components such as ICE and multi-gear transmissions.; thereby eliminating the majority of the operating costs. However, EV purchasing costs might be considerably high because of costly batteries [5]. Fig. 1.2 illustrates the operating and purchase costs of different vehicle types [6-7].

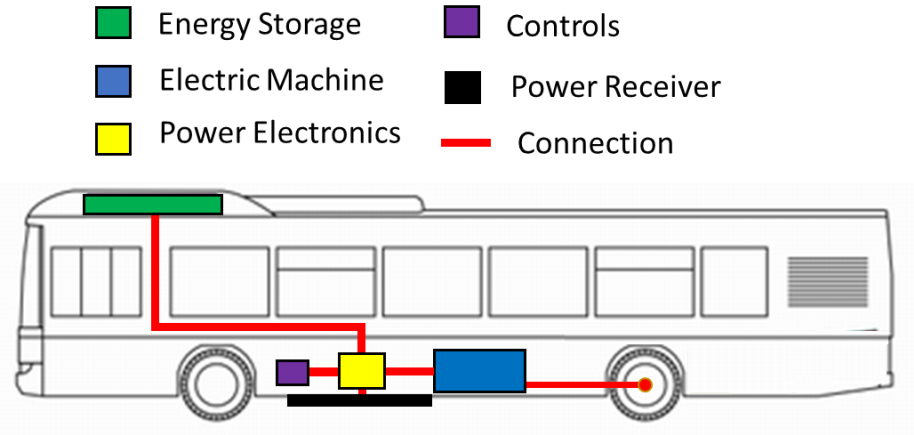

Figure 1.1: EV system components.

Methods for reducing the costly battery size of EVs have been, and continue to be, studied. The most common method is to charge the vehicle when it is idling or not in use [8]. Another method proposes battery-swapping stations that allow EV buses to visit the stations on route and change their batteries [9]. Fortunately, one pattern, called 'opportunity charging,' not only reduces the battery size but also allows it to be fast-charged while the bus is on the go [8]. 'Opportunity charging' means to charge the battery at each opportunity. Instead of depending on the charge at the end of the route cycle, the 'opportunity charging' pattern allows charging the bus batteries whenever it stops at the bus-stop while disembarking and boarding passengers. Thus, reducing the required battery size for each driving cycle. This pattern is already getting adopted by a number of institutions. One example is the iconic red buses of the London Transportation System that plan to use electric buses and adopt the 'opportunity charging' technology [9]. Although the technology is challenging and still immature, it is safe to conclude that electric based bus networks are to be a part of future cities.

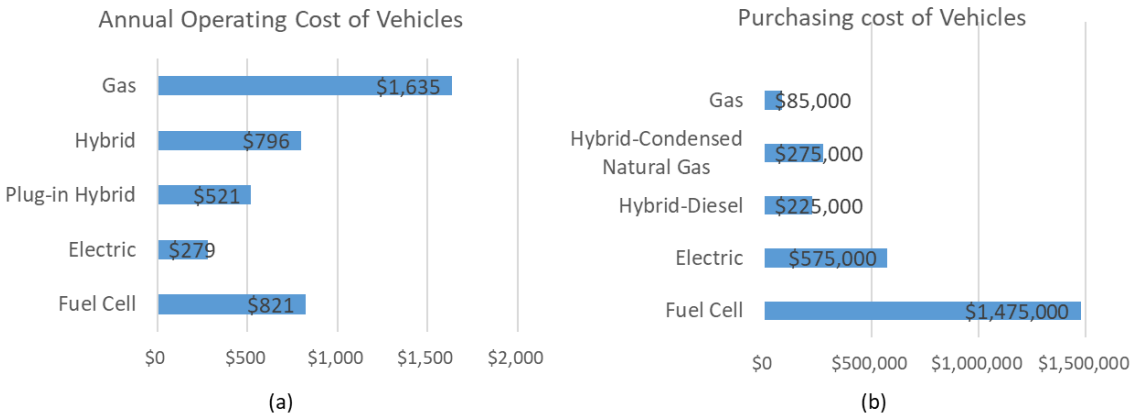

Figure 1.2: (a) Annual operating cost of different types of vehicles. (b) Cost of acquiring different types of electric buses.

One of the major challenges of bus networks that rely on EV technology is to plan the route schedule so that the batteries do not drain completely while on duty. Especially, for an EV bus network powered by opportunity charging, planning a schedule might be an enormously difficult task because of varying conditions such as weather conditions and traffic slow-downs while minimizing energy consumption. It would also be ideal to charge the vehicle no more than what would be needed to get to next bus stop by predicting the required amount of energy and time depending on the route and vehicle conditions.

The other challenge would be the low energy efficiency of EV systems. For this purpose, the energy efficiency of EVs must be investigated. The power dissipation on EV components can be divided into four main categories: impulsive unit losses (such as electric machine), power electronics unit losses (inverters, converters), loss of the battery power, and mechanical losses (transmission, differentials, wheels, etc.), which depend upon varying vehicle parameters and route conditions such as the road grade, number of passengers, speed limits, traffic updates and weather conditions. Thus, the energy consumption of an EV bus network can be reduced by adapting the vehicles and the schedule to reduce power dissipation.

Although many limitations of the EV technology are eliminated, problems such as low efficiency levels, long charging period, and short driving range are still the main obstacles. Electric buses require fast charging and long driving range to meet their schedule requirements. Therefore, the innovative charging technologies and driving cycle optimizations are required to achieve these targets.

1.2. Thesis Objectives

This thesis aims to improve the operating system efficiency of EV buses to ease the penetration of the technology into the public transportation arena. This work proposes a cost-optimized solution for EV based city transportation ensuring minimal energy consumption along the route considering the road grade, number of passengers, speed limits, traffic updates and weather conditions. According to the proposal, recently updated data about the route conditions is considered to be used by the speed and charging profile optimizer (which could be a computer), and the speed and charging profile are optimized using an optimization method and sent to the electric buses and the bus stops. Hence, the optimized data is used to drive and charge the vehicles optimally, thereby reducing the energy consumption of the bus network. Figure 1.3 demonstrates overall driving path and the operating conditions.

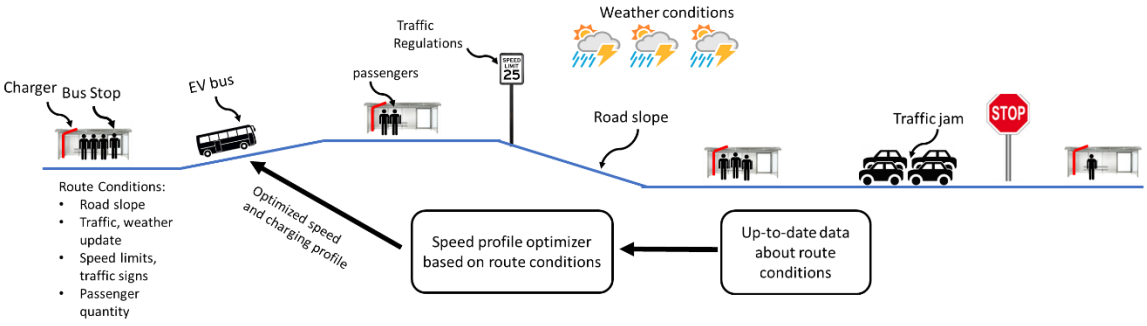

Figure 1.3: Proposed bus network topology and its optimization.

An ‘opportunity charging’ city bus network is investigated, so the electric buses are considered to be charged at each bus-stops while disembarking and boarding the passengers. To consider the battery degradation impact of the opportunity charging, a battery degradation model which included battery parameters such as depth of discharge (DOD), state of charge (SOC), and operating temperature.

In order to determine the energy consumption impact of the route conditions, an example electric bus that is exposed to route conditions is modeled and simulated. An optimal size electric machine and inverter are specified and simulated, considering possible scenarios, to ensure that they work at peak efficiency as much as possible.

Eventually, a multi-objective optimization problem that considers the energy consumption, the battery degradation, and the bus schedule is formulated. To optimize the driving cycle (or speed profile) and the charging profile, a Particle Swarm Optimization (PSO) algorithm is applied to the system since it works well at solving multi-objective optimization problems.

CHAPTER II

LITERATURE REVIEW

This chapter summarizes the literature review of selected topics related to the work being proposed in this thesis. The main areas of the literature that apply to this thesis are vehicle energy consumption models, powertrain technology, optimization methods, energy storage technologies, and electric bus networks charging patterns. A vehicle model is required to determine the energy consumption for varying route conditions while a powertrain topology must be specified for energy consumption simulations. EV energy storage types are also investigated for battery cost predictions purposes. Since the aim is to optimize an electric bus network, charging patterns for electric bus networks are investigated, including their advantages and disadvantages. Once a thorough understanding of the issues involved is gained, an optimization method that fits the problem is selected.

2.1. Vehicle Model

An electric bus is considered and simulated for energy consumption in this study. Thus, an energy consumption model for the considered vehicle is required. The methods presented in the literature are typically based on vehicle mechanics. Therefore, the amount of energy required to take a vehicle from point ‘A’ to point ‘B’ is calculated using motion dynamics principles. The fundamentals of motion dynamics are derived from Newton’s second law of motion, which relates force to mass and acceleration. The law states that an object accelerates proportionally when the summation of the applied forces is nonzero [10].

In case of a vehicle, there are four forces that work against or for the motion: tractive force (F_{TR}), rolling resistance (F_{roll}), aerodynamic drag force (F_{AD}), and gravitational force (F_{gxT}). Rolling resistance, aerodynamic drag force, and gravitational force works against the motion and called road load forces while the tractive force works for the motions, as depicted in Fig. 2.1. In an EV, the tractive force is generated by the electric machine in the vehicle. Rolling resistance occurs whenever the road is not flat, or the wheel is not rigid, while aerodynamic drag is caused by air friction. The gravitational force is the result of the gravitation on earth [12].

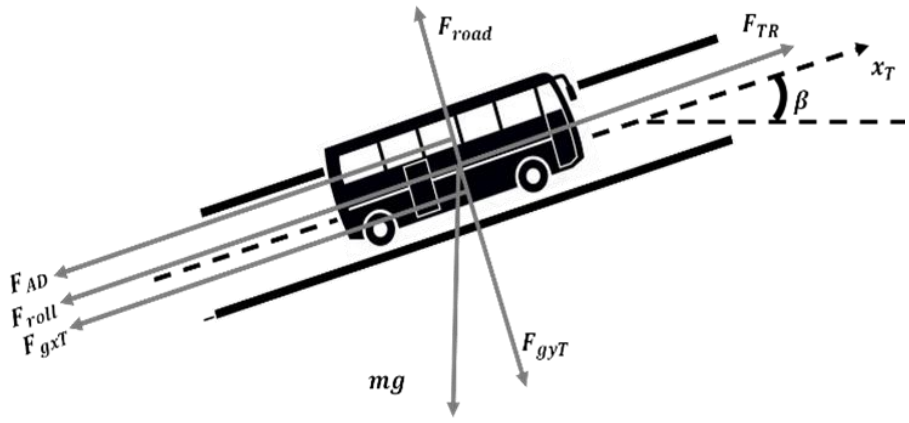

Figure 2.1: Free body diagram of a vehicle.

In [13], an energy consumption model based on classical mechanics is developed and tested on some routes. In that model, the rolling resistance is given as:

$$F_{roll} = m\ g\ f_r \tag{2.1}$$

where, m is the vehicle's mass, g is the gravitational acceleration, and f_r is the tire rolling resistance coefficient. The aerodynamic drag force is calculated as:

$$F_{AD} = 0.5\rho C_D A_F (v + v_{wind})^2 \tag{2.2}$$

where, ρ is the air mass density, C_D is the aerodynamic drag coefficient, A_F is the frontal area of the vehicle, v is the vehicle speed, and v_{wind} is the wind velocity. The gravitational force is calculated as following:

$$F_g = mgsin(\beta) \tag{2.3}$$

where, m is the vehicle mass, g is the gravitational coefficient, and β is the road slope angle. The difference between the forces that move and stop the vehicle generates acceleration as follows:

$$F_{TR} - F_g - F_{roll} - F_{AD} = m\,a \tag{2.4}$$

where, a is the acceleration. Based on classical mechanics, the energy required to move the vehicle a certain distance *x* is:

$$E = F_{TR}\,x \tag{2.5}$$

where, E is energy in Joules. In [13], the EV model based on (2.1-2.5) was tested for different driving scenarios and proved to be satisfactory, as the results are shown in Fig. 2.2. In the figure, the four different scenarios are shown on the left; these driving scenarios have varying routes and lengths. On the right, energy consumption results are shown for both simulation and test drives; the routes with longer route lengths have more energy consumption in Joules.

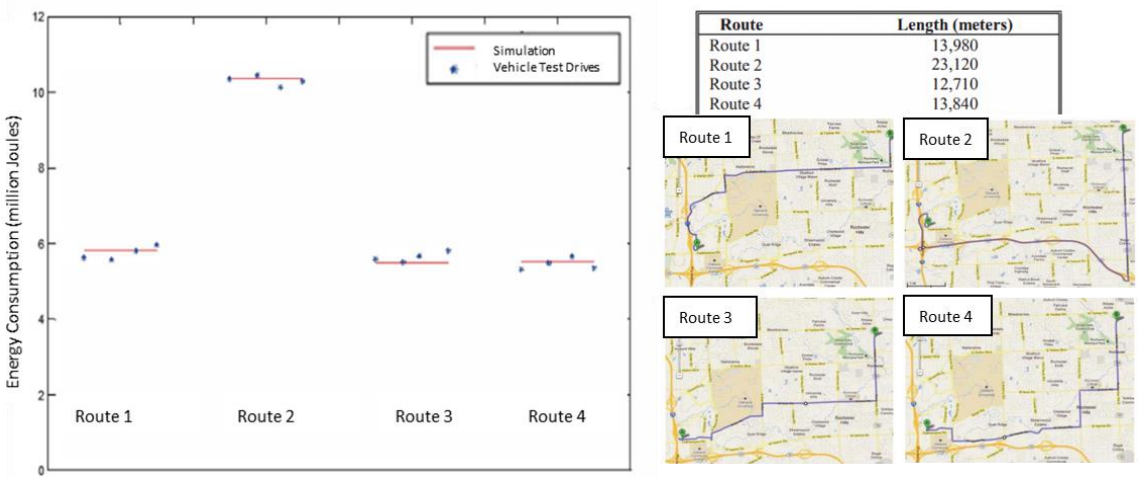

Figure 2.2: Energy consumption results of test and simulation for different routes considered.

There has been a significant amount of work devoted to calculating the vehicle's energy consumption for varying route conditions. Depending on classical mechanics, an accurate range estimation considering road grade, road conditions, and wind speed has been developed [14]. However, while the results of [15] agree with those of other similar studies [15,19] only a few studies have included traffic updates in their predictions [16]. Similarly, the authors of [18] predicted EV power requirements in some scenarios where they considered road grade, road and air conditions. Although they ignored time-dependent factors such as traffic jams and weather conditions, the results are still satisfactory. On the other hand, predicting driver behavior for energy consumption might not be accurate since the study in [15] suffered from inaccurate results when predicting driver behavior's effect on energy consumption.

Even though it has yet to be validated via test results by many researchers [16-19], the accuracy of the physical mechanics equations for determining energy consumption is considered high in the literature.

2.2. Vehicle Powertrain Technology

Powertrain design is another factor that contributes to the energy consumption characteristics of EVs. Powertrain refers to certain vehicle components like electric machines, transmission, differentials, and wheels that play a major role in the vehicle motion. EVs and ICE vehicles have different powertrain units. Table 2.1 compares the powertrain components in the two systems [11], [12].

Table 2.1: Comparison of conventional and electrical powertrains.

Conventional Powertrain	**Electrical Powertrain**
Internal Combustion Engine (ICE)	Electric Machine
Transmission with multiple gear ratio**s**	Transmission with a single gear ratio
Generator for 12 V loads	Converter for 12 V loads
Fuel tank	Battery

In the literature, two types of powertrain architectures are mainly studied for hybrid/electric vehicles: parallel and series. Upcoming sections describe both architectures and compare their advantages and disadvantages.

2.2.1. Parallel Powertrain Architecture

Both the ICE and electric machine work together in a parallel architecture. Both run simultaneously and generate power to propel the wheels through either a single or a multi-gear transmission, as shown in Fig. 2.3. On one hand, the advantage of this design choice is that it allows design engineers to use a smaller electric machine and ICE for a performance similar to that of the series architecture. On the other hand, the parallel architecture is complex to implement and requires a complex mechanical coupling device such as a clutch between the electric machine and ICE for mechanical power transfer [12].

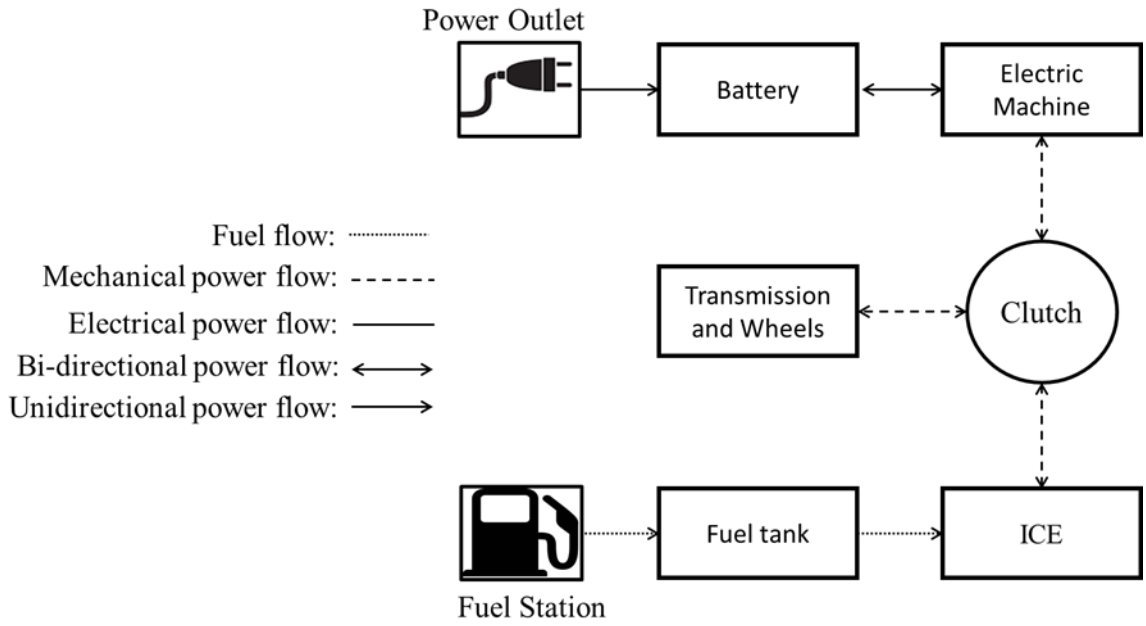

Figure 2.3: Parallel vehicle architecture.

2.2.2. Series Architecture

Besides parallel, the series architecture is commonly adopted by manufacturers. In a series architecture, the ICE is mechanically disconnected from the wheels, and the battery can be charged via an electric machine, a power outlet, or ICE as shown in Fig. 2.4. The greatest advantages of the series design are its simplicity and ability to use solely the electric machine for short trips such as inner-city transportation. Because power is delivered only by the electric engine, it must produce the torque required for high load driving scenarios [12].

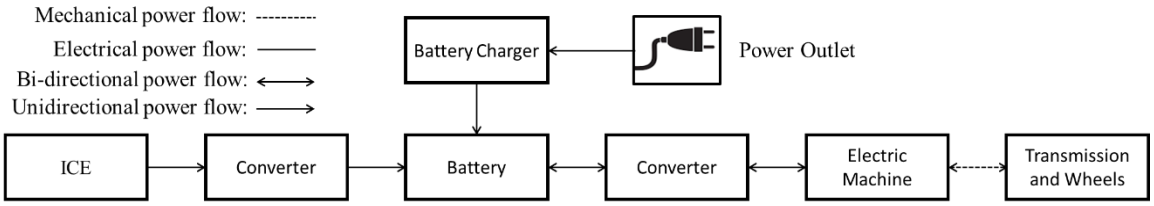

Figure 2.4: Series architecture.

The series powertrain design might differ based on the EV application. Driven by performance expectations, EVs can have more than one electric machine [2]. In Figure 2.5, possible drive train implementations are shown for varying applications [12]. In Fig. 2.5(a), the design has four machines, one for each wheel; the design might be advantageous because it allows usage of smaller size machines. However, it creates the problem of speed and torque synchronization among the machines. In Fig. 2.5(b), the design enables motion of the vehicle in case that one of the machines fails because the two machines at the front are mechanically connected. In Fig. 2.5(c), regenerative braking does not take advantage of the braking force at the front wheels because there is no motor connected to them. In Fig. 2.5(d), the design has only one machine; thus, it is easy to implement because there are no multiple motors that create complexity and incur extra costs [2, 11-12].

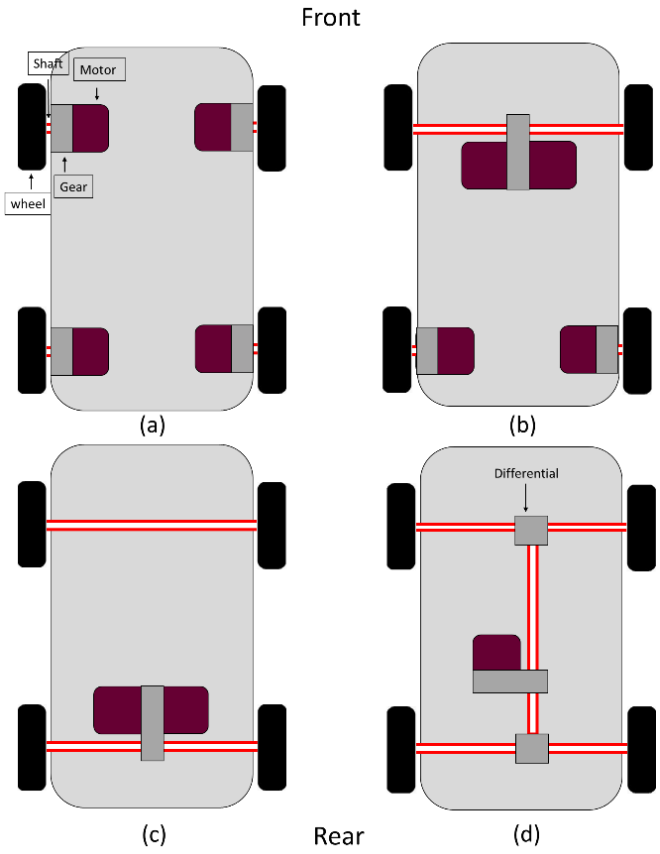

Figure 2.5: Possible powertrain designs for EV bus application. a) Four-wheel drive with four motors. b) Four-wheel drive with four motors with a front differential. c) Rear wheel drive only. d) Four-wheel drive with one motor.

2.2.3. Electric Machine Selection

The electric machine is the most important part of the hybrid-electric vehicle (HEV) powertrain. It not only generates propulsion but also generates electricity during braking. The electric motor must also work efficiently at low speed and high torque applications such as an electric bus. The other criteria for selecting an electric machine are power density, costs, and reliability. The previous researches have conducted analyses comparing permanent magnet synchronous machines (PMSM), induction machines (IM), switch reluctant machines (SRM), and direct current machines (DC) for EV applications [20-22].

The DC machine enjoys of low manufacturing cost and high technical maturity. It also offers less complex power electronics units. However, for power levels higher than 20kilo Watts, it requires a complex winding design [20]. Furthermore, it does not provide sufficient reliability and low maintenance costs. Therefore, the disadvantages of DC machines are below the high requirements of EVs [20].

On one hand, IMs are technically mature and offer higher power density and better efficiency compared to DC machines, especially at high speeds. On the other hand, IMs are less efficient compared to PMs, and they require complex control algorithms to achieve good performance [21].

SRMs provide higher power and torque densities and better efficiencies compared to IMs. However, they require a complex converter design for high torque production and suffer from torque ripple and acoustic noise issues [22].

PMSMs offer higher power and torque densities and better efficiency compared to other machine types. Furthermore, PMSMs works more efficient at higher torque levels compared to IMs and SRMs while SRM and IM work more efficient at high speeds. Figure 2.6 provides the efficiency comparison of different machine types. The efficiency areas that are more than 85 per cent are highlighted for the three different machine types [20]. Vehicles require significantly higher torque during start-ups, which is the case for inner-city driving cycles. As a result, PMSMs might be a suitable choice for energy saving EV applications. However, it is a costly design choice because of high magnet prices.

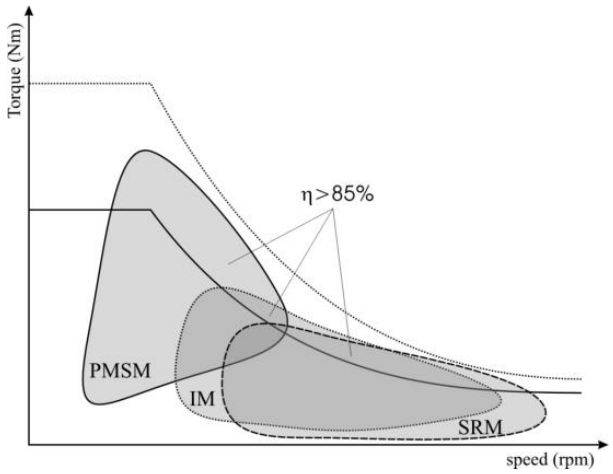

Figure 2.6: Efficiency maps of different machines.

The advantages and disadvantages of the electric machines mentioned above are summarized in Table 2.2 [20, 23].

Table 2.2: Evaluation of the electric machine types.

Criterion:	DC	IM	PMSM	SRM	Legend
Power Density	- -	*	++	*	++: very good
Efficiency	-	+	++	+	+: good
Cost	+	++	-	+	*: neutral
Reliability	-	++	*	+	-: bad
Technical Maturity	+	+	*	*	--: very bad

2.3. Battery Storage

One of the main obstacles to EV adoption is the cost of the energy storage units. ICE vehicles have dominated the market because of their convenience in storing energy. The electric bus industry requires high power and energy density along with a considerable amount of efficiency and long-life cycles. Among the available types of batteries, the four types of batteries considered for the industry expectations are as follows:

- Nickel-metal-hydride (NiMH)
- Sodium Sulfur (NaS)
- Lead-acid
- Lithium-ion

Battery features such as power and energy density, efficiency, and life cycle are investigated [12]. Power density means the charging or discharging power per unit amount of battery weight that the battery can handle, while energy density means battery capacity per battery unit. Energy efficiency is affected by the internal resistance of the battery during charging and discharging. The cycle life is the number of times a battery can be charged before it losses 30 percent of its capacity. These features for different battery technologies are compared in Table 2.3. Considering industry expectations, Lithium-ion batteries are chosen as the energy storage element for the electric bus in this study because they possess the best power density and efficiency, and second-best energy density and good life cycle [12].

Table 2.3: Properties of EV batteries

Battery Type	Energy Density (Wh/Kg)	Power Density (W/Kg)	Energy Efficiency (%)	Life Cycle (Count)
Lithium-ion	90-160	200-350	>90	500-1000
NiMH	60-80	200-400	70	1000-2000
Sodium Sulfur	150-240	230	85	1000
Lead-acid	35-50	150-400	80	500-1000

Although Li-ion batteries have been used in EV applications for the last several decades, their energy storage density has yet to reach a satisfactory level. Additionally, their low power capacity causes long charging periods and thus the lack of power supply

at peak demand. Consequently, solutions are required to increase power and energy density of EV storage systems, or on how to use the available limited storage more efficiently.

A feasible solution for the EV high-power demand is the use of ultra-capacitors. They are very useful for high power applications and may prove convenient for EVs during peak power demand, such as when the vehicle is taking off because batteries cannot support instant load changes. High power demand from batteries leads to battery degradation as it causes both a high depth of discharge (DOD) and high temperature [24-26]. The literature has much to offer on hybrid storage systems composed of ultra-capacitors and Li-ion batteries [27]. However, this configuration fails during long trips with a high percentage road graded road because while ultra-capacitors provide high power for a short time, they lack energy density. Low energy density results in larger ultra-capacitor arrays, requiring more space and increasing weigh on the vehicle. Moreover, the hybrid storage configuration does not solve the issues associated with the long charging period of electric buses [28].

The second problem of the energy storage systems is their low energy density. This problem is forcing the industry to add more battery weight to EVs in order to extend their range. A higher battery weight increases the overall vehicle weight, leading to a heavier load on the electric machine; thereby diminishing energy efficiency and causing undesirable mechanical consequences. This study aims to ease this problem by introducing the opportunity charging pattern to city bus networks. This approach reduces the required battery capacity and long charging periods while increasing the frequency with which the battery is charged. However, increasing the battery charging frequency will, over time, decrease the lifetime expectancy of the battery. This issue has been investigated in the

literature ([24], [25]) to predict battery degradation effects of DOD, state of charge (SOC) and temperature. Further, battery degradation models have also been developed. Using these models to simulate charging and discharging scenarios have proven to significantly increase battery life [38]. In this thesis, a battery degradation model is adopted to define the impact of battery degradation on the above-mentioned parameters [37-38]. The battery degradation model is given in details in Chapter 3.

2.4. Charging Patterns for Electric Bus Networks

Electric city bus networks are still in their early stage of development. The battery storage problems result in high operating costs. Even the most advanced storage technologies fail to solve two major problems; namely, the “long charging time” problem because of insufficient power density, and the “high weighed storage system” problem because of low energy density. Thus, researchers have focused their efforts on charging topologies.

There are two schemes proposed in the literature: battery swapping and on-board charging, as shown in Fig. 2.7. [27-29]. Battery swapping technologies rely on high capacity batteries to be swapped at the end of every route cycle. The main advantage of this method is that it allows the batteries to be charged slowly, resulting in increased battery lifetime. However, this method requires high capacity, heavier, and bigger size batteries, thereby increasing the battery cost and thus the overall system cost. The extra investment required by typically complex battery swapping schemes is likely to increase the cost of the bus network [30].

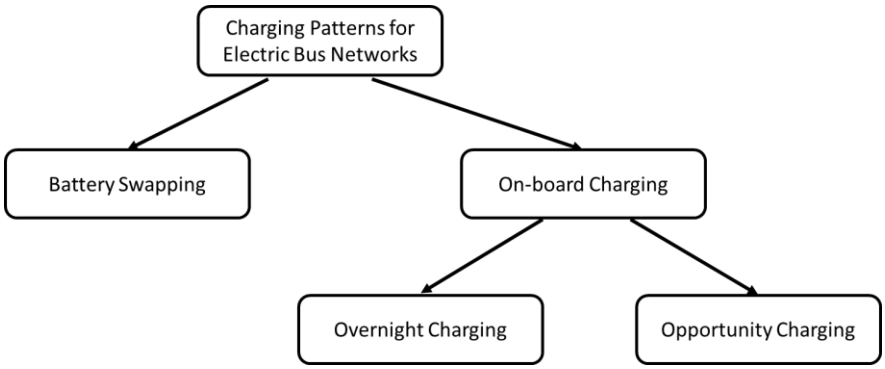

Figure 2.7: Charging schemes for electric bus networks.

The other method is to do on-board battery charging. Since this method increases the number of charging cycles, researchers are focusing their attention on developing optimal charging methods.

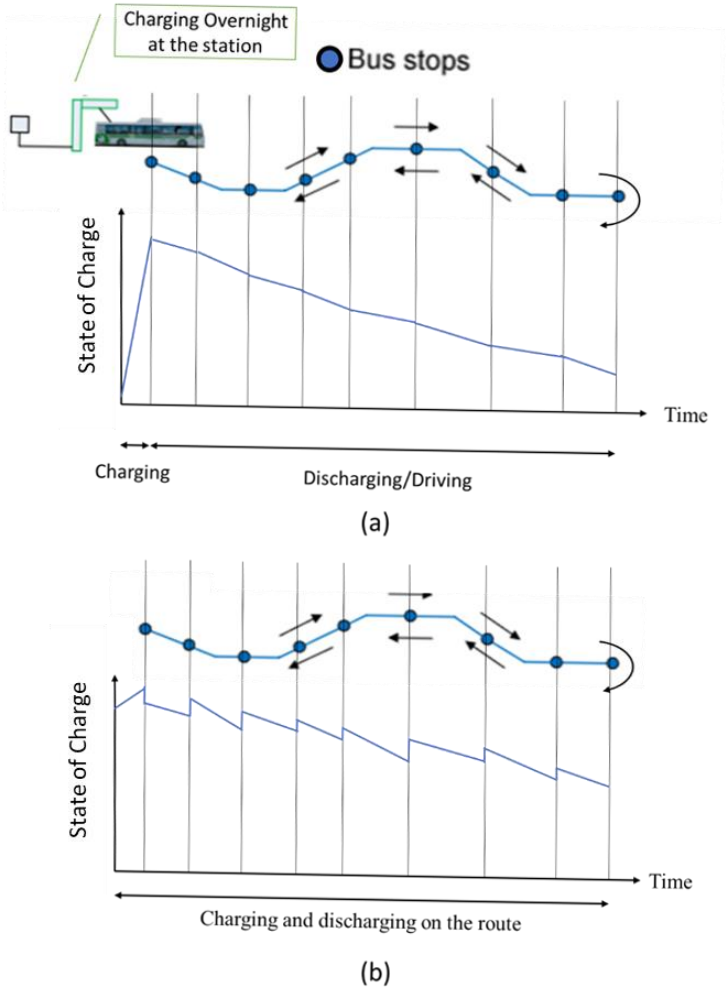

Figure 2.8: Overnight charging topology with battery SOC levels. a) Overnight charging. b) Opportunity charging.

There are two different on-board battery charging concepts: opportunity charging and overnight charging. Since overnight charging, shown in Fig. 2.8-a, relies on charging the vehicle every night, it requires a relatively bigger battery size and longer charging time. Opportunity charging, on the other hand, which means charging the EV at each bus stop, requires a lower battery capacity on the bus and a high-power charger system in each bus stop [26]. Unlike personal vehicles, transit EVs are used with fixed routes and schedules; as a result, they take advantage of shorter battery charging periods and optimizing the

charging pattern to ensure lower operating costs and longer battery life, thereby making them cost-effective for inner city applications [8].

2.5. Optimization Methods

The aim of the optimization problem is to minimize the energy consumption of an electric bus network by optimizing the speed and charging profile. Optimization methods in the literature were investigated to decide an optimization algorithm. Investigated methods are Linear Programming (LP), Dynamic Programming (DP), the Genetic algorithm (GA), and Particle Swarm Optimization (PSO) as categorized in Fig. 2.9.

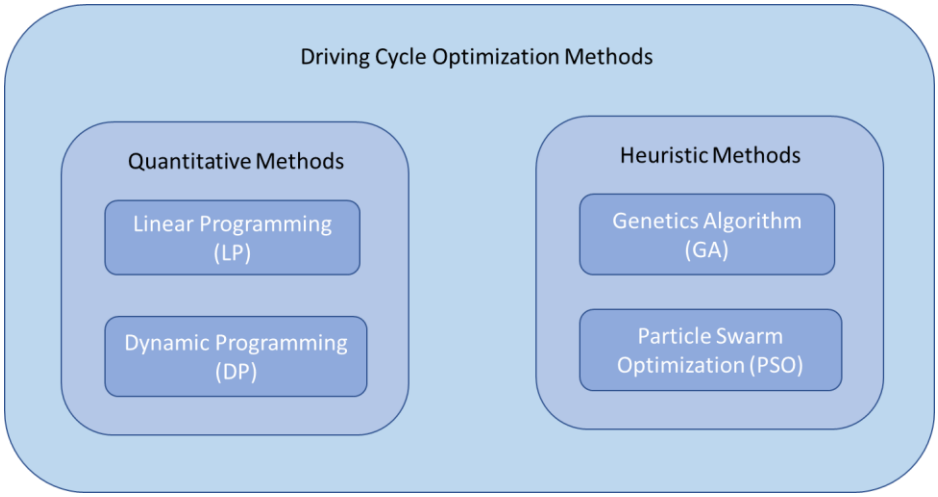

Figure 2.9: Driving cycle optimization methods.

2.3.1. Linear Programming

LP is frequently used for linearly formulated problems for battery charging applications. For driving cycle optimization, it might be desirable to use experimental energy consumption data, which might lose their characteristic when linearly formulated. The disadvantage of this method is that it requires problem linearization, which may cause system characteristics to be lost [31].

2.3.2. Dynamic Programming

DP is used to discover the shortest path between two points. For instance, the shortest path between point *B* and point *H* is highlighted in Fig. 2.10. This approach can be applied to driving cycle optimization problems. The points can be assumed to be road segments, while paths can be assumed to be the speeds between the road segments; thus, there would be a large number of paths and points. However, it is not practical to apply DP to problems with many variables and parameters since it requires a huge deal of computation power and memory. It may eventually lead to long processing time [32].

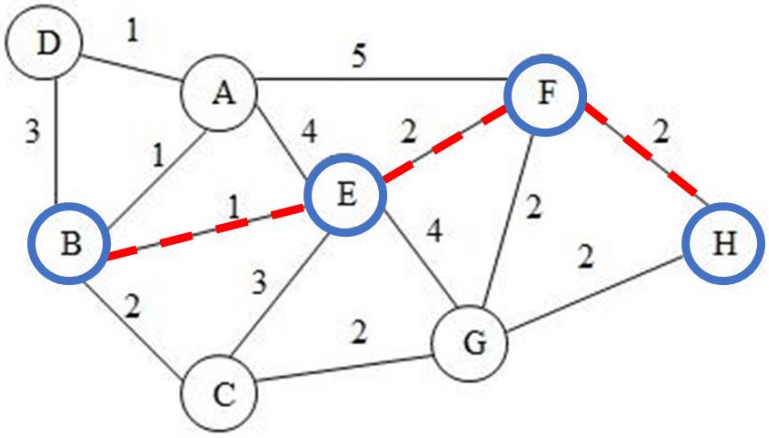

Figure 2.10: Shortest path between point B and H or vise-versa.

2.3.3. Genetic Algorithms

GA are inspired by the Evolution Theory. This iterative method imitates the natural selection method [33]. GA has five stages: initialization, selection, crossover, mutation, and termination. It starts with the initialization stage where initial species are generated randomly. Then, these species undergo a natural selections process during the selection stage, so that the strong species (the ones giving better optimization results) survive while others die. In the third stage, the species interchange characteristics and generate new

individuals which undergo a random mutation; this stage ensures that the next generation of species is stronger than the previous ones. This process repeats itself until a satisfactory generation of species is produced, as described in Fig. 2.11. The process stops at the termination stage. GA is well-suited to solving multi-objective optimization problems [33].

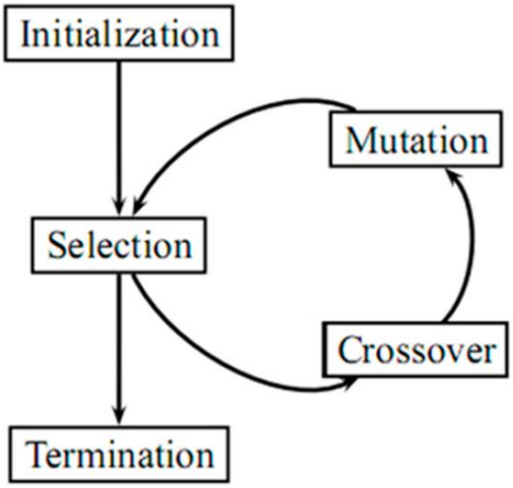

Figure 2.11: Stages of GA.

2.3.4. Particle Swarm Optimization

The first researchers who discovered the power of PSO in multi-objective optimization problems are Parsopoulos and Vrahatis [33]. Since then, PSO has been widely used to solve many multi-objective problems [34-35]. In this thesis, a multi-objective optimization problem is defined, as explained in Chapter 3. PSO is widely used for power systems optimization problems. It is a population-based method that only relies on the "objective" evaluation. Within the population, the particles, which have varying velocities, move in the space as they aim to get close to the optimal point, as shown in Fig. 2.12. The velocity of each particle decreases as the optimal points are reached. Unlike GA, which uses competition among the species, PSO takes advantage of the cooperation among particles to approach the optimal point. Moreover, PSO is easy to implement and only a

few parameters need to be adjusted. It has no evolution operators such as crossover and mutation [36]. In many studies, PSO has been found useful for energy management and efficient driving applications [31, 19]. Consequently, PSO is chosen as the optimization algorithm here because of its superior performance, compared to that of GA, in multi-objective optimization problems [37].

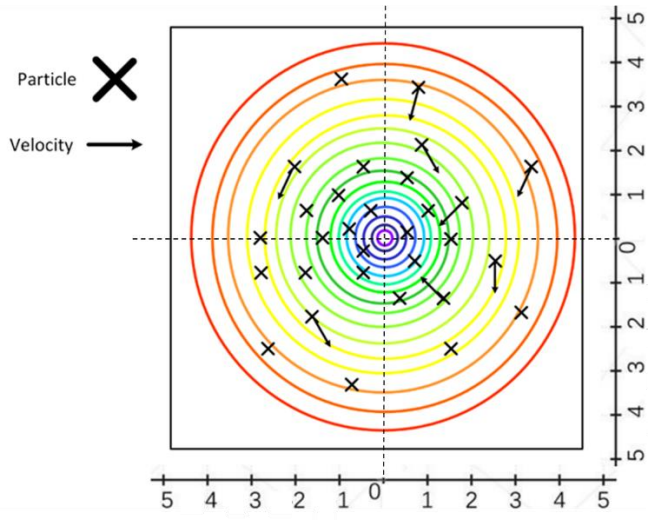

Figure 2.12: Particles and their velocities in PSO.

2.3.5. Driving Cycle Optimization

Cities in many parts of the world have complex bus networks, with fixed schedules, that include EV buses and conventional buses with drivers. Many previous studies [38-40] developed techniques that suggest how to reduce energy costs while running EVs. Since recent developments in computer science and communications allow computers to use real-time traffic and weather update data to optimize the speed profile of city bus networks, this work proposes an autonomous, computer-driven bus network that attempts to optimize as many objectives as possible to further reduce energy consumption and battery cost. According to [34], autonomous vehicle design might reduce peak power by 35% and required total energy by 28%.

A number of driving cycle optimization methods have been developed for different applications and scenarios. Some optimization-based studies focus on deterministic strategies [32], while others focus on computational methods [31]. Also, several authors have approached this optimization problem with adaptive dynamic programming, which controls the system online and learns its characteristic over time, [39-41]. However, since common bus networks run on a fixed schedule, their characteristic is rigid and known. In [33], a transit vehicle scheduling driven by a GA-based method to optimize the costs is presented. The drawbacks are short range and long recharge time [33]. The study in [35] also proposes a GA-based method with a battery swapping depot where batteries are stored and charged when idle. However, battery swapping is a complex task; thus, they propose a powerful robotic system to remove the high-weighted batteries form the vehicles, a process that takes up to 15 minutes. In contrast, this thesis aims to solve the driving cycle optimization problem by integrating the opportunity charging pattern with a PSO algorithm to ensure that a short range and a long recharge time, and complex battery swapping systems are not a problem.

The fixed bus schedule is another factor that must be considered in the optimization problem because energy consumption is very sensitive to running time. A specified travel time for the certain route may result in a high vehicle velocity which, in turn, leads to higher road resistance causing the electric engine to consume more energy. With that in mind, only a few studies included timing problems in their work. Even so, these authors did not consider time-dependent issues such as traffic updates and weather conditions [42].

This work aims at considering most of the parameters that might affect the bus network timing and schedule. For this reason, the bus schedule, traffic regulations, and wind speed are considered for the optimization problem.

2.6. Conclusions

This chapter covers the literature review about the study in the thesis. The related literature is categorized into five main sections: vehicle energy consumption models, powertrain technology, optimization methods, energy storage technologies, and electric bus network charging patterns.

In the vehicle model section, the subsection of the vehicle for energy consumption are investigated. An energy consumption model based vehicle mechanics is introduced. The accuracy of the existing models is discussed.

Existing vehicle powertrain technologies are presented for an EV design. Therefore, series and parallel vehicle architectures, and their advantages and disadvantages are discussed.

Battery Storage technologies are presented to develop models for the battery degradation cost. Different types of battery technologies are discussed, and their features are compared in a table.

Charging patterns proposed in the literature to solve the long charging time problem of the electric buses are presented and compared.

Finally, optimization methods are investigated for solving the optimization problem defined in Chapter 4. The optimization methods such as PSO, GA, DP, and LP are investigated in their individual sub-sections for determining the most feasible method.

CHAPTER III

SYSTEM PRESENTATION AND SIMULATION

The components of the EV bus are investigated for design optimization purposes. The EV bus design considerations that have a major impact on the overall cost of the network are its drivetrain components. In this case, an EV bus has three main electrical components: electric engine, power electronics, and storage systems. Mechanical parameters of the vehicle are also design considerations for the optimization problem. In this chapter, the vehicle components and parameters are specified, and the vehicle model is simulated, which are required for driving cycle and charging profile optimization.

The energy consumption on varying route conditions is simulated in this chapter. Specifically, the simulation components such as motor drive system, vehicle mechanics, battery degradation, powertrain, driver models, and route conditions are covered in details. Eventually, the models are integrated into the simulation (Section 3.5, Figure 3.10). MATLAB/Simulink is used as the simulation tool, and the results are presented.

3.1. Electric Machine Drive System

An efficiency map of a motor drive system is considered for the energy consumption simulation. This system is specifically built for EV applications by an industrial company. The motor electric drive system consists of a Brushless Permanent Magnet Motor (PMSM), an inverter, and an internal controller as shown in Fig. 3.1. The

motor drive system can be driven via its user interface and be controlled using one of its modes: speed, torque. and analog control modes.

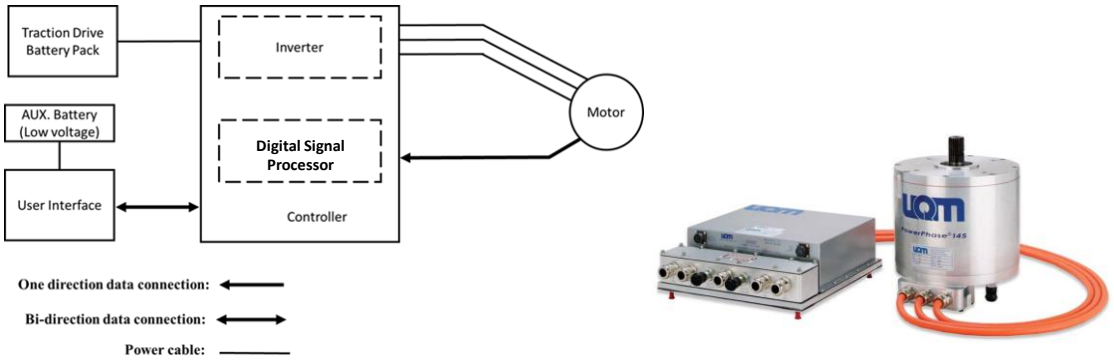

(a) (b)

Figure 3.1: (a) Block diagram of electric vehicle drive system. (b) A visual of the electric vehicle drive system.

The motor drive system is considered as the propulsive unit in the powertrain design (specified in the next section). However, the drive system in the vehicle is only simulated for its energy consumption. Accordingly, the efficiency map of the system is acquired and used in the simulation. The motor drive system is tested experimentally, and the losses for all operating points are measured as described in Fig. 3.2. The system was run in speed control mode, and the load torque was increased gradually, allowing its efficiency to be acquired for each operating point. Eventually, results are modeled using a look-up table.

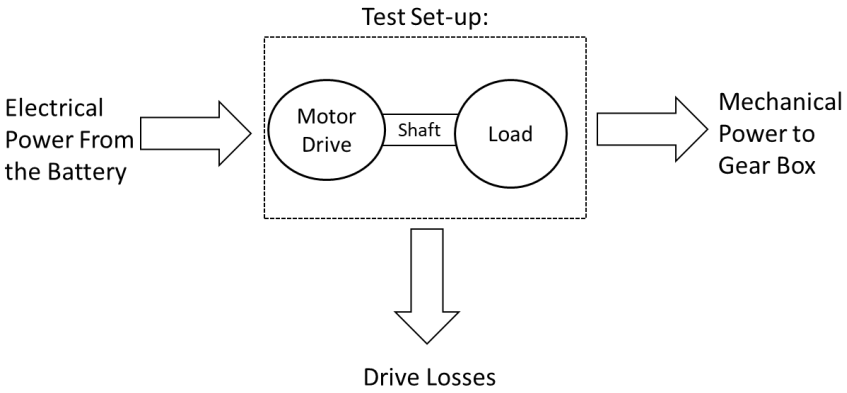

Figure 3.2: Motor drive system test set-up.

the experimental test results are acquired from dynamometer set-up at The University of Akron. The efficiency map of the drive system is presented in Fig. 3.3. The Efficiency points are interpolated using MATLAB/Simulink curve fitting and interpolation toolbox to include it into the vehicle simulations.

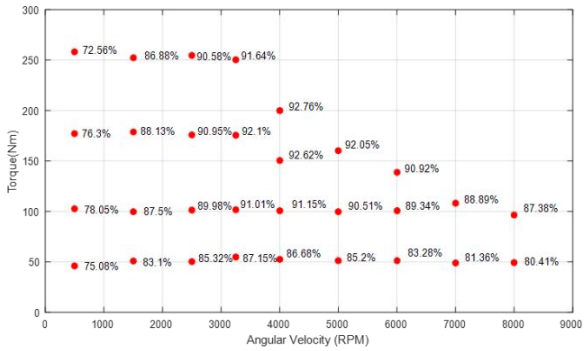

(a)

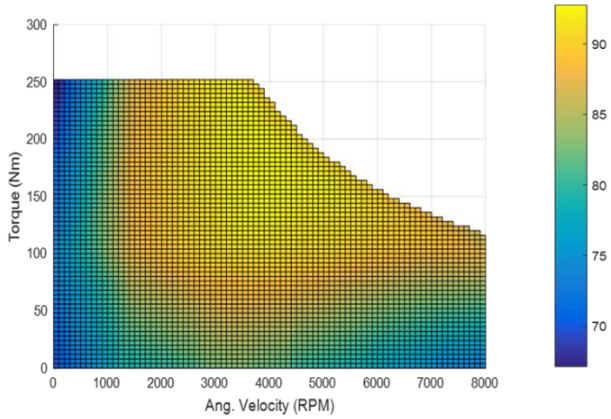

(b)

Figure 3.3: Efficiency map of the motor drive system. (a) Tested operating points and their efficiency. (b) Interpolated efficiency map.

3.2. Vehicle Model

A vehicle model must be specified for the energy consumption calculation. The vehicle model considered in this study is investigated in two parts: the vehicle powertrain and the vehicle mechanics. The EV powertrain can be described as the mechanical and electrical power interconnections. EVs might have varying powertrains such as parallel and/or series. Using vehicle mechanics, the vehicle dynamics which resulted from the forces applied to the vehicle are calculated. Using the vehicle dynamics, the energy consumption of the vehicle on certain route conditions is determined. The vehicle powertrain and the vehicle mechanics are presented in the next sections.

3.2.1 Vehicle Powertrain

Although the aim of the study is not to design a state of the art EV, the vehicle powertrain is specified for energy consumption purposes. In Chapter II, two powertrain architectures were reviewed [11-12] namely, parallel (Fig. 2.2) and series (Fig. 2.3). Their advantageous and disadvantages were discussed. Since this study aims to reduce the overall cost of the bus network, the series architecture was selected because of its simplicity, low cost, and easy implementation. Unlike the common series architecture [12], ICE is not considered to run during trips, but it is meant to be used for charging the batteries when there is no plug-in charging available [11-12]. The electric machine is connected to the four wheels v differentials and a single-gear transmission. The four-wheel drive enables a better regenerative braking performance because the braking force is divided among the four wheels. With four-wheel drive, all the braking force applied to the vehicle can be used to regenerate energy because there is no conventional breaking (braking pads, rotors etc.). As a result, the considered design consists of a series connected battery pack, inverter, electric machine, gearbox, differentials, and wheels as shown in Fig 3.4

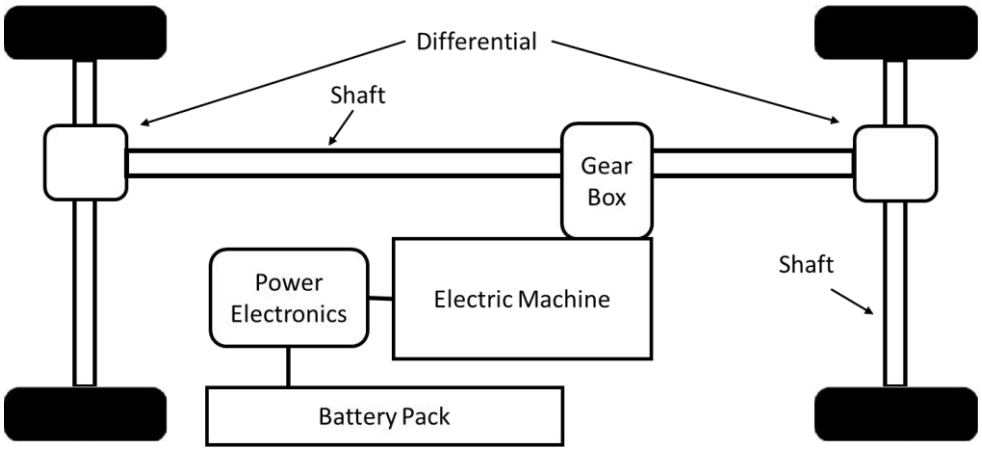

Figure 3.4: Description of the powertrain considered in the study.

The powertrain parameters such as wheel radius, vehicle mass, gear ratio, and machine power are also specified. The wheel radius and mass are typical for electric buses; the electric machine power is already specified as 100 kW previously. The gear ratio is the ratio of the diameters of the gears in the gearbox. Table 3.1 shows the powertrain sizing parameters of the vehicle.

Table 3.1: Powertrain sizing of the vehicle.

Description:	**Value:**	**Unit:**
Vehicle Mass	1900	kg
Gear Ratio	1:8	-
Wheel radius	0.32	meter
Machine Power	100	kW

Powertrain equations are defined based on the specified powertrain design in Fig. 3.4 and used in the simulation that is covered in the following sections. Therefore, the following equations relates the machine torque to the tractive force and vehicle speed to machine speed.

The following equation relates the machine torque to the tractive force.

$$F_{TR} = T_m \frac{GR}{wr} \tag{3.1}$$

where, F_{TR} is the tractive force, T_m is the machine torque, GR is the gear ratio, and wr is the wheel radius. The other equation relates vehicle speed to machine speed.

$$w_m = v_{xT} \frac{GR}{wr} \tag{3.2}$$

where, v_{xT} is the vehicle speed, and w_m is the motor speed.

3.2.2 Vehicle Mechanics

A vehicle mechanics model is required for the energy calculation. In this thesis, an EV bus is simulated to determine its energy consumption on a certain route. The vehicle mechanics model is derived to simulate route conditions, as mentioned previously. The impact of the route conditions on energy consumption is determined by the road load forces which work against the vehicle motion. From Chapter II (Eqns. 2.1-2.4), there are three road load forces: rolling resistance (F_{roll}), aerodynamic drag coefficient (F_{AD}), and gravitational force (F_{gxT}), as depicted in Fig. 2.1. The tractive force (F_{TR}) that causes the motion is generated by the electric machine [12]. The vehicle mechanics model is investigated in the literature and expanded upon as more parameters and constants are added to determine the effects of the varying route conditions on energy consumption. The final version of the model is as follows:

The tractive force equation must be developed depending on the vehicle powertrain. This force is generated by the traction unit of the vehicle, and the magnitude is determined by the powertrain, as specified in Eqn. (3.1).

Rolling resistance always works against the motion. As shown in Fig. 3.5, a flattening tire or deformation on the road surface moves the instantaneous center of rotation toward the direction of the motion.

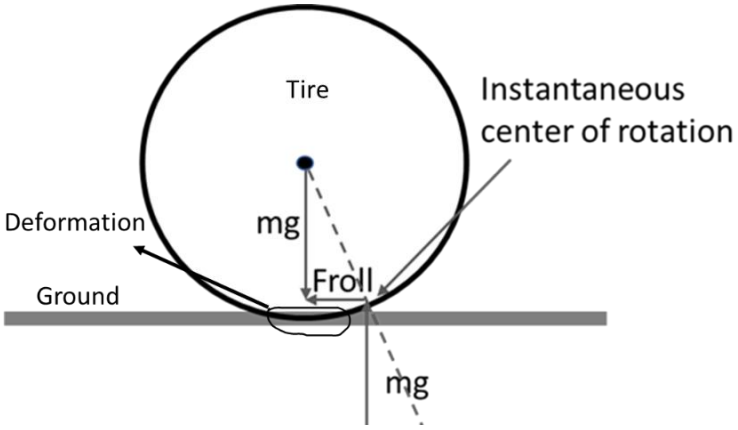

Figure 3.5: Rolling resistance force occurred on a wheel.

The rolling resistance force, which must be overcome to be able to break the tires free and start moving the vehicle, is described as [12] and given by:

$$F_{roll} = sgn[v_{xT}]mgcos\beta(C_0 + C_1 v_{xT}^2) \tag{3.3}$$

where, C_0 and C_1 are rolling resistance coefficients, β is the slope angle, v_{xT} is the vehicle velocity, m is the vehicle mass, g is the gravitational coefficient.

The aerodynamic drag force also always works against the motion, and it is calculated as:

$$F_{AD} = \text{sgn}(v_{xT})\{0.5\rho C_D A_F (v_{xT} + v_0)^2\} \tag{3.4}$$

where, ρ is the air density, C_D is an aerodynamic drag coefficient, A_F is the frontal area of the vehicle, and v_0 is the wind velocity.

Unlike the aerodynamic drag force, the gravitational force may or may not work against the vehicle motion based on the sign of slope angle β, and calculated as follows [13]:

$$F_{gxT} = mgsin(\beta) \tag{3.5}$$

Summing the rolling resistance, aerodynamic drag, and gravitational forces gives the so-called road load force, described as:

$$F_{RL} = F_{gxT} + F_{roll} + F_{AD} \tag{3.6}$$

The difference between the tractive and road load forces causes motion of the vehicle, giving rise to acceleration as follows [11]:

$$v_{xT} = \int \frac{F_{TR} - F_{RL}}{m} dt \tag{3.7}$$

The tractive power (P_{TR}) is:

$$P_{TR} = F_{TR} v_{xT} \tag{3.8}$$

Finally, the energy consumption is calculated as:

$$e_{TR} = \int_{t1}^{t2} \frac{P_{TR}}{E} dt \tag{3.9}$$

where, e_{TR} is energy in joules, E is the efficiency of the motor drive system, and t_1 and t_2 are integration intervals.

The energy consumption of the vehicle is determined by the equations 3.1-3.9 and the coefficients used for the energy consumption calculation is given in Table 3.2 [12].

Table 3.2: Coefficients used for the vehicle model.

Description	Symbol	Value	Unit
Frontal Area	A_F	2	m^2
Air mass density	ρ	1.17	kg/m^3
Rotational inertia coefficient	k_m	1.1	-
Gravitational acceleration	g	9.81	m/s^2

The other parameters such as the road slope angle (β), vehicle mass (m), the rolling resistance coefficients (C_1, C_0), wind velocity (v_0), aerodynamic drag coefficient (C_D) are considered as the route conditions, as they are covered in the following section.

Vehicle mechanics are used in EV simulations to determine the route conditions' impact on the EV energy consumption.

3.2.3 Route Conditions

Vehicle mechanics allow engineers to determine the energy consumption of a vehicle under certain route conditions. The route conditions are simulated as constants or coefficients in the vehicle mechanics equations that are given previously. Specifically, there are five different route conditions considered in this study:

- Road grade
- Number of passengers
- Road conditions
- Wind velocity
- Ambient air condition

A. Road Grade:

Road grade is the percentage angle of the road. For instance, if the road angle is zero, the road grade is zero percent. If the angle is 90 degrees, then the angle is 100 percent. Road grade is modeled as the road slope angle (β).

B. Number of Passengers:

The number of passengers has an impact on total vehicle mass. As the number of passengers increases, the vehicle mass (m) increases, therefore, the rolling resistance and the gravitational force also increase. In this thesis, each passenger is assumed to weight 60 kg.

C. Road Conditions:

Different types of roads (such as asphalt, concrete, gravel, etc.) define the road conditions and the rolling resistance coefficients (C_1, C_0). If the road is less rigid, then it increases the magnitude of the rolling resistance force and the energy consumption.

D. Wind Velocity:

Wind velocity (v_0) might either help or go against the movement of the vehicle, depending on its direction. There might be wind blowing or not depending on some segments of the road.

E. Air Conditions:

The physical conditions of outside air affect air friction. Air parameters such as humidity and temperature impact the aerodynamic drag coefficient of the air, so the air conditions are considered as aerodynamic drag coefficient (C_D).

All the route conditions and their coefficients mentioned above have an impact on road load forces (Eqn. 3.3-3.5). The first route condition, road grade, relates to two road load forces: gravitational force and rolling resistance. The number of passengers only impacts the overall mass of the vehicle and contributes to gravitational and rolling resistance like road grade. The route condition, called road conditions, only impacts the magnitude of the rolling resistance. The last two route conditions are about the outdoor air, which is affected by temperature and humidity [12]. The wind velocity may work for or against the motion, and it affects the aerodynamic drag force. The aerodynamic drag coefficient is used to simulate the physics of the air. The rolling resistance and aerodynamic drag force (Eqn. 3.3, 3.4) are affected by the vehicle speed, which is determined by the vehicle dynamics based on the difference between the road load forces and the traction force (Eqn. 3.7). Figure 3.6 describes the route conditions and their role in the vehicle model.

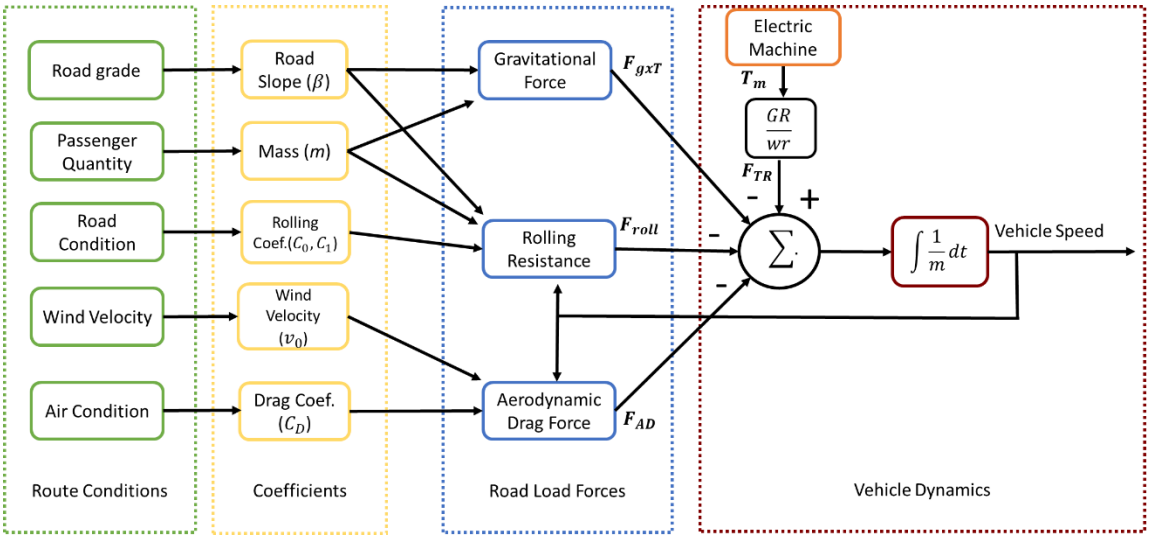

Figure 3.6: Role of the route conditions in EV energy consumption.

In the EV simulation, the route conditions block contains the route-condition coefficients as a function of the vehicle location. All five coefficients are modeled as look-up tables as shown in Fig. 3.7.

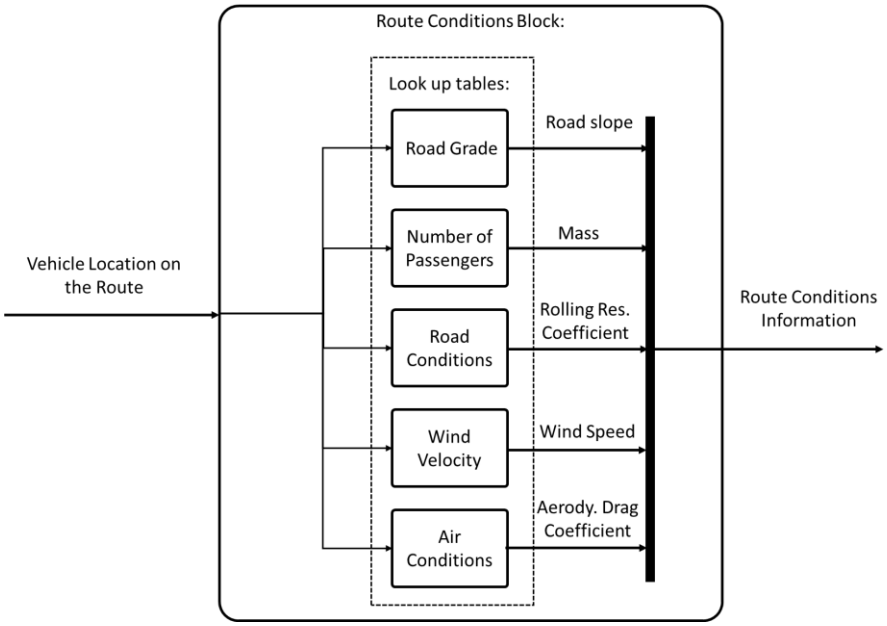

Figure 3.7: Route conditions block.

3.3. Battery Degradation Model

Battery fade or degradation costs occur during both driving and charging the vehicle. Therefore, battery aging factors are analyzed and represented in the formulation of the optimization problem. However, battery degradation prediction is a complex task as the various factors affecting the aging are unpredictable. Three different factors such as the state of charge (SOC), the depth of discharge (DOD) and the battery temperature are typically considered in the literature as battery aging factors [24-26].

Temperature changes due to high battery charge or discharge reduce battery life. Battery temperature is strongly related to the battery average power P_B, as given by the Arrhenius relation

$$T = T_{amb} + R_{th}|P_B| \tag{3.10}$$

where, T is the battery temperature, T_{amb} is the ambient temperature of the battery pack, and R_{th} is battery thermal resistance. The Arrhenius equation describes the temperature impact on battery life [24]. A high battery temperature reduces not only the battery capacity but the battery power also. Equation (3.11) shows the relationship between battery temperature and battery lifetime.

$$L(T) = aQe^{\frac{bQ}{T}} \tag{3.11}$$

where, L is the battery lifetime, and Q is battery capacity, a and b are curve fitting coefficients. Thus, the battery degradation cost is determined by integrating the temperature impact over time. The cost is formulated in (3.12), where *Yhr* is a constant that stands for the amount of time the battery is used in a year, and C_{bat} is the battery price. The lifetime of a battery is considered to be over when the battery capacity reaches 30 percent of its initial capacity.

$$C_{temp} = C_{bat} \int_{ti}^{tf} \frac{dt}{YhrL(t)} \tag{3.12}$$

Another factor that contributes to a diminishing battery lifetime is SOC. Particularly, it refers to the percentage of available charge left in the battery. SOC can be written as follows:

$$SOC(t) = \frac{Q_a(t)}{Q_r}\ 100 \tag{3.13}$$

where, Q_a is the available charge left in a time t, Q_r is the total charge capacity of the battery. Computational SOC modeling is a complex task. Accordingly, this model has been

made possible using experimental data from the literature. Equation (3.14) is developed using a curve fitting method [25].

$$C_{SOC} = C_{bat} \frac{mSOC_{avg} - d}{Q_{fade} nYhr} \tag{3.14}$$

here, Q_{fade} is the capacity fade, *m*, *d*, and *n* are curve fitting constants.

Unlike SOC, DOD refers to the percentage electric charge or discharge amount at a specific event as described in

$$DOD = \left| \frac{SOC(t_{end}) - SOC(t_{start})}{Q_r} \right| 100 \tag{3.15}$$

here, t_{start} and t_{end} are the start and end times of the event, respectively. Battery degradation resulting from DOD is given by (3.16).

$$C_{DOD} = \frac{C_{bat}}{2N\ DOD\ Q\ u^2} \tag{3.16}$$

here, *u* is the efficiency rate of discharging/charging, and *N* is the number of battery cycles for a specific DOD. The battery degradation cost is determined by the dominant factor [25].

$$C_B = \max(C_{DOD}, C_{SOC}, C_{temp}) \tag{3.17}$$

3.4. Driver Model

A driver model is used to drive the EV at a certain speed. The vehicle speed controller should be able to eliminate the steady-state error between actual and reference vehicle speed. Therefore, a PI (proportional and integral) controller is designed to control the speed of the modeled vehicle as shown in Fig. 3.8, where K_p is the proportional and K_i is the integral controller.

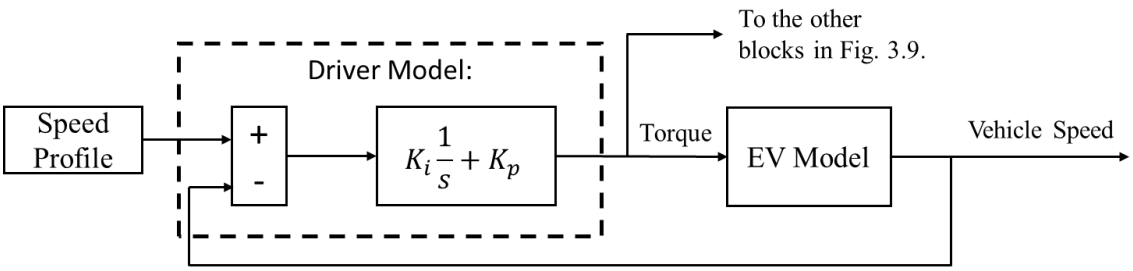

Figure 3.8: Driver model used to drive the vehicle.

3.5. Simulation of the EV Bus

An efficiency map of the motor drive system (considered as the propulsive unit of the EV) is acquired and already shown in Fig. 3.3. Thus far the route conditions and their impact on energy consumption have been identified, the powertrain and its sizing have been specified, the driver model has been given, and the battery degradation model has been discussed. In this section, these results are combined in order to simulate battery degradation and energy consumption costs.

The driver model takes the speed profile from the user to set the actual speed and determine the required amount of torque using the driver model block (Fig. 3.8). The vehicle model takes the torque command from the driver block, and the route conditions provided by the route conditions block to determine the vehicle speed (Eqn. 3.3-3.7). The vehicle speed history is used to determine the actual EV location by providing the route conditions block, which has the look-up tables for various route conditions, to determine the coefficients for the vehicle dynamics.

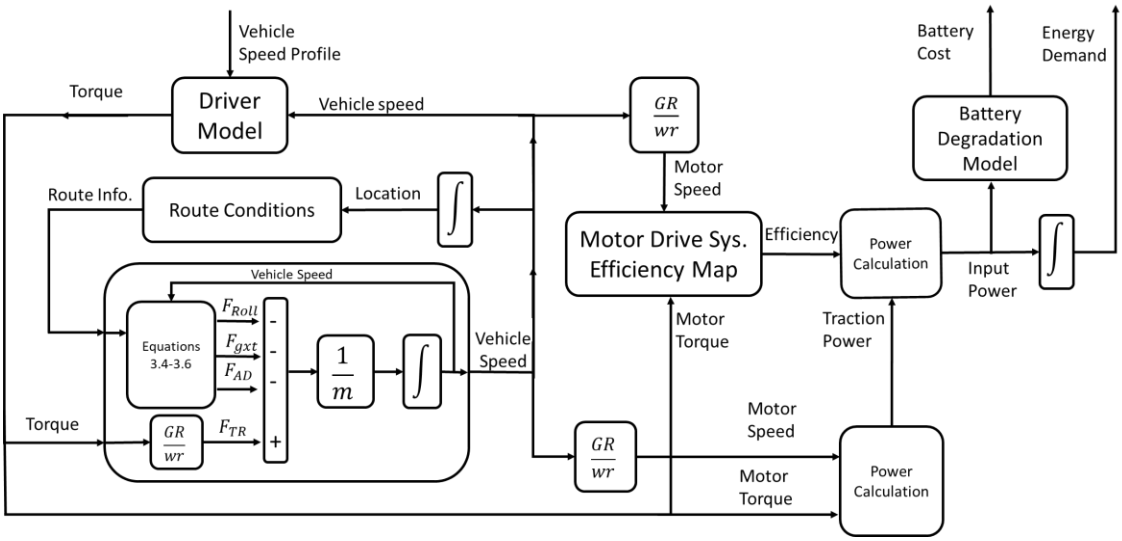

Figure 3.9: Electric vehicle model used to determine its energy demand (energy consumption) and battery cost.

Vehicle speed is converted to the motor speed through Eqn. (3.2). The motor speed, from the gearbox block, and the torque output, from the driver model block, are provided to the motor drive block to determine the efficiency of the motor drive system as well as the power required by the battery. Both instantaneous and historical battery power consumption are used to determine energy consumption, or demand, (Eqn. 3.8-3.9) and the battery degradation cost (Eqn. 3.17) as described in Fig. 3.9.

In summary, the vehicle simulation blocks take the speed profile from the user and determine the energy demand and battery degradation cost.

3.6. Simulation Results

The simulation results are made possible using the vehicle parameters previously mentioned. Equations (3.1-3.8) and the vehicle constants are used for the vehicle model. For the powertrain, the design shown Fig. 3.4, the constants in Table 3.1, and Equations (3.1-3.2) are used. The efficiency map of Fig. 3.3 is also used in the simulation. As for route conditions, only road grade is simulated here. The road grade is used to calculate the

road load forces (Eqn. 3.6). The vehicle simulation in Fig. 3.9 was run for varying vehicle speeds over 0.05 miles. Therefore, the energy consumption is calculated using Eqn. (3.8-3.9). The simulation was run for three different road grades: 0, 5, and 10 degrees. The results are shown in Fig. 3.10.

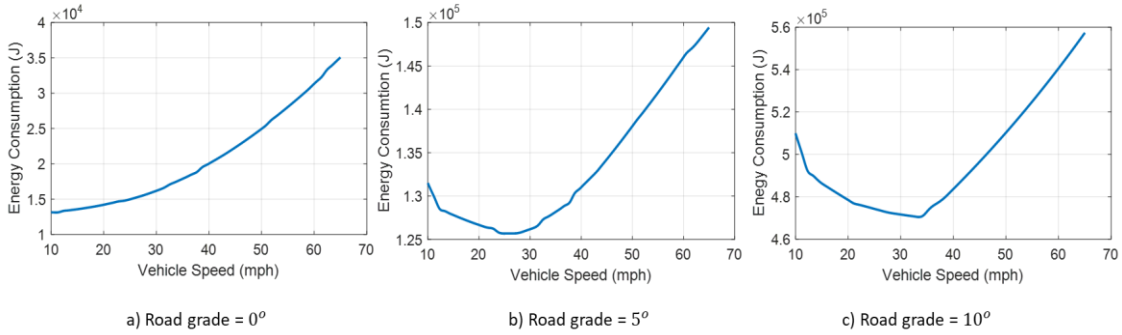

Figure 3.10: Simulation result for different road grades. a) Road grade = 0^o . b) Road grade = 5^o. c) Road grade = 10^o.

As seen in from the above simulation results, the optimal vehicle speed that yields minimal energy consumption is different for different road grades, which is expected. This feature of EVs allows engineers to optimize the vehicle speed so that the overall efficiency of the vehicle can be increased. The optimization algorithm covered in Chapter IV takes advantage of this feature to optimize the driving speed of the electric bus and thus reduce the overall cost of the bus network.

3.7. Conclusions

This chapter specifies and simulates the EV considered in the optimization problem. Accordingly, an electric motor drive system efficiency is acquired, and the efficiency map is modeled using MATLAB/Simulink. Then, an electric bus model is defined and simulated with the motor drive system for energy consumption under specific route conditions. A battery degradation model is used to determine battery fade. Therefore,

the energy consumption and battery degradation cost are obtained. In Chapter IV, energy consumption and battery degradation are considered as the costs of the bus network and used to optimize the overall efficiency and cost of the bus network.

CHAPTER IV

OPTIMIZATION

In Chapter III, the electric vehicle (EV) bus energy consumption dynamics and battery degradation model are given. Also, energy consumption data and battery degradation estimations were obtained. In this chapter, these results are used to optimize the speed profile of the EV bus route and the bus charging, at each stop, to achieve lower operating costs. This is referred to as the "optimization problem." A Particle Swarm Optimization (PSO) algorithm is developed to solve the optimization problem.

4.1. Problem Formulation

The city bus network with opportunity charging requires that vehicles be charged at each bus stop. Thus, the bus network considered in this thesis is divided into two phases: the driving phase and the charging phase. During the driving phase, two types of costs are investigated: the electrical energy consumed and the battery fade during traveling. During the charging phase, when the bus stops at the bus stop, there is only a battery degradation cost because the vehicle speed is zero. A third cost is the penalty cost, which results from violating the bus schedule. The problem formulation is explained next.

A. Charging Phase Cost:

Charging phase cost occurs at the bus stop when the vehicle is being charged. Since the charging power is high; the charging cost is considerably higher than the battery cost

during driving. Hence, the charging phase cost is equal to the battery degradation cost C_B (Eqn. 3.17).

B. Driving Phase Cost:

The driving phase cost C_R refers to the costs incurred while driving between two bus stops. It is the sum of the energy consumption cost (C_E) and the battery degradation cost during travel (C_B).

$$C_R = C_E + C_B \tag{4.1}$$

The vehicle model equations used for calculating the energy consumption (e_{TR}) has already been explained in Chapter III. So, the cost of energy consumption is calculated as:

$$C_E = e_{TR} ET \tag{4.2}$$

where, ET is the eelectricity tariff ($/kwh). The battery degradation cost (C_B) is calculated as the dominant factor using the battery degradation model (3.16) given in Chapter III.

C. Penalty Cost:

Most city bus networks have fixed driving cycles, so buses must reach a specific destination at a specific time. However, optimizing the driving speed/cycle for minimal cost might disrupt bus schedules and impact the entire bus network schedule. In order to tackle this problem, a penalty function is introduced in the optimization problem. The penalty function adds a cost whenever the schedule constraint is violated. If the bus reaches the bus stop right on time, penalty function value is zero, as shown in Fig. 4.1.

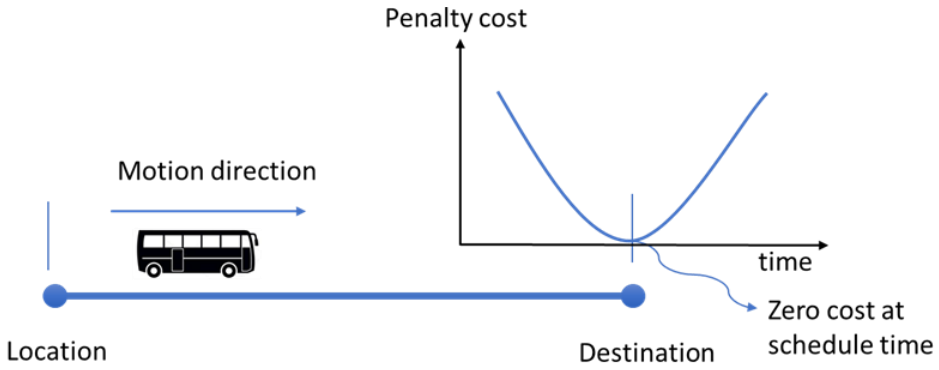

Figure 4.1: Implemented penalty function.

The penalty function is chosen to be parabolic to increase schedule flexibility and decrease sensitivity for small scheduling errors. The cost function is formulated as

$$C_P = S(t_{arrival} - t_{sch})^2 \tag{4.3}$$

where, $t_{arrival}$ is the actual arrival time, t_{sch} is scheduled arrival time, and S is a constant that defines how important the bus schedule is. S must be a large number whenever the bus schedule is firm. Figure 4.2 shows how different types of costs contribute to the global cost of the system. Notice that two models and a penalty function are used to calculate the overall cost of the bus network. The weights of the energy consumption, battery, and the penalty costs are governed by the electricity tariff, battery price, and penalty constant respectively.

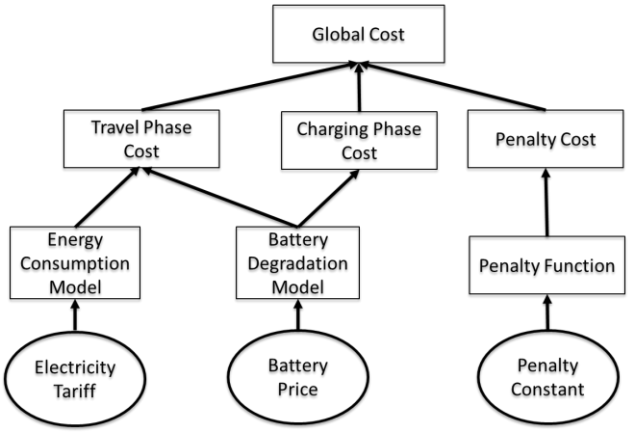

Figure 4.2: System costs and their contribution to the global cost.

The bus route is divided into two phases namely driving and charging phase. The driving phase is divided into a hundred intervals while the charging phase is considered as one interval. The vehicle can operate with different velocities at each interval. Depending on the route conditions, the cost functions for each interval will vary. The global cost of the system (C_G) is the sum of costs of all the intervals as following:

$$C_G = \min \sum_{i=1}^{i=I} [C_R(i) + C_B + C_P] \tag{4.4}$$

where, C_G is global cost, i is interval, and I is the number of intervals, which is 101.

4.2. PSO Algorithm

An optimization algorithm is developed to solve the optimization problem posed in Eqn. 4.4. The power of PSO is that is well suited for multi-objective optimization problems. Its advantages over other methods, such as genetic algorithm, are covered in the literature review. The bus route is divided into 101 intervals. One hundred intervals are reserved for the driving phase to determine the optimal driving cycle, and one interval for the charging phase. Since the bus network is assumed to have a strict bus schedule, the bus is expected to reach its destination on time. That is, if an interval speed increases then the other interval speeds should decrease to compensate accordingly. Thus, the speed of an interval has an impact in the optimal speed of the other intervals. Accordingly, the optimization problem is defined as a multi-objective optimization problem with 101 objective functions. As mentioned before, PSO is a powerful tool for multi-objective optimization problems.

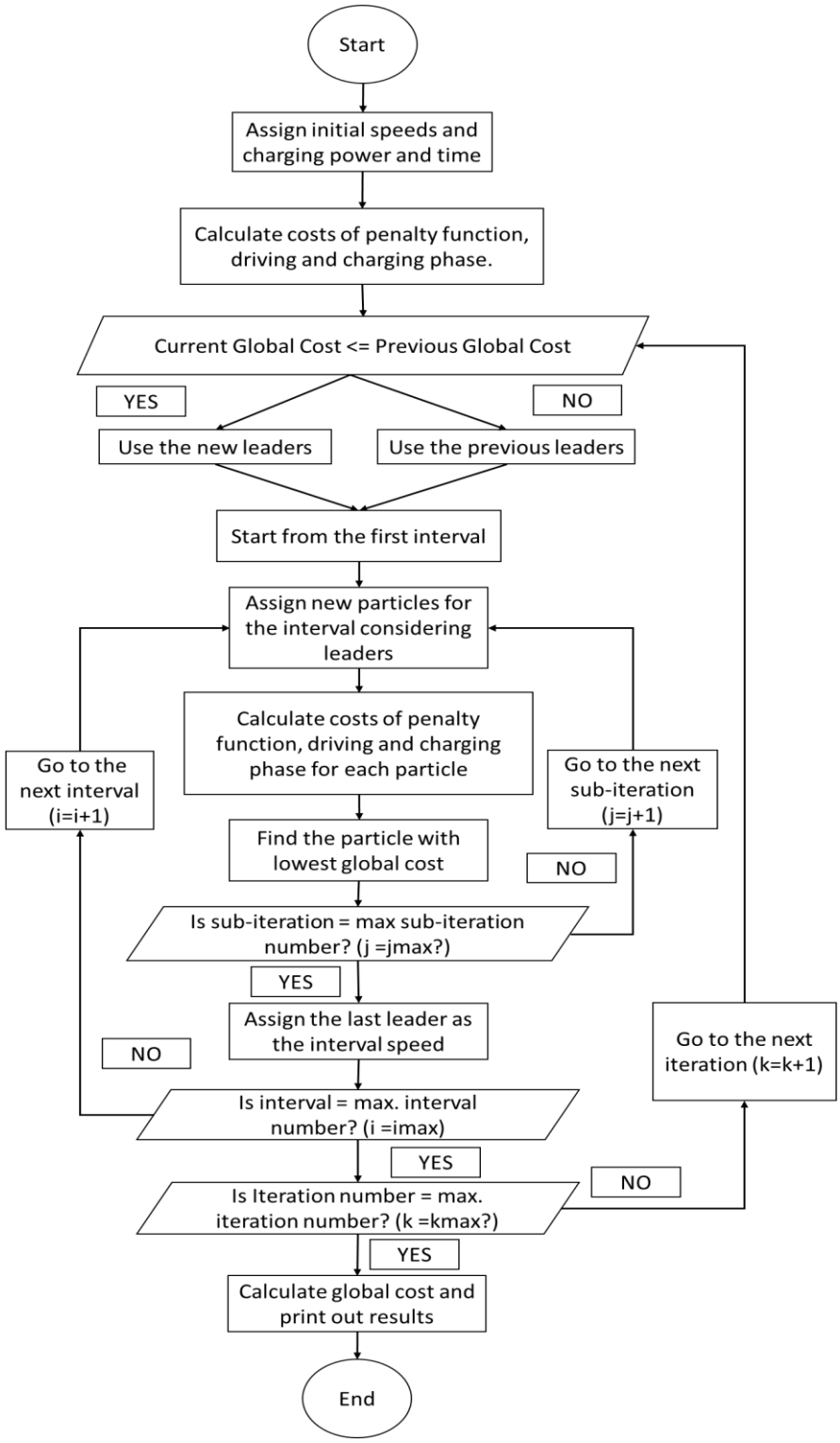

Figure 4.3: Developed PSO for driving cycle optimization.

To solve the multi-objective optimization problem, a specific PSO is applied. The algorithm starts by assigning an initial speed to each interval along the route. It then calculates the energy consumption of each interval and the battery degradation cost. The sum of the interval times is the arrival time of the bus to the bus station, where the vehicle gets charged. The outcome of the penalty cost function is governed by the difference between the arrival time and the scheduled time. Finally, the algorithm calculates the global cost of the system as the sum of the driving phase costs, the charging phase costs, and the penalty cost. At the next iteration, the PSO generates particles; each particle represents different speeds at an interval. Thus, the program starts with the first interval and calculates the global cost for each particle of the interval, it then switches to the next interval and repeats the same process for each interval in one iteration. For the next iteration, the same process is repeated. New particles are created for the intervals based on the best particle (leader) of the same interval in the previous iteration. The global cost is calculated and the leaders of all of the intervals are updated. An example of the global cost and an interval leader are shown in Fig. 4.4, as the number of iterations increases during the optimization process. This process is made possible by three nested loops. The outer most loop is `k`, which is the iteration number. The middle loop is `i`, which defines the route interval number (from zero to 101), and the inner-most loop, `j`, is the iteration number for each interval. The three nested loops make the PSO method feasible for solving multi-objective optimization problems. The developed PSO algorithm is described in Fig. 4.3.

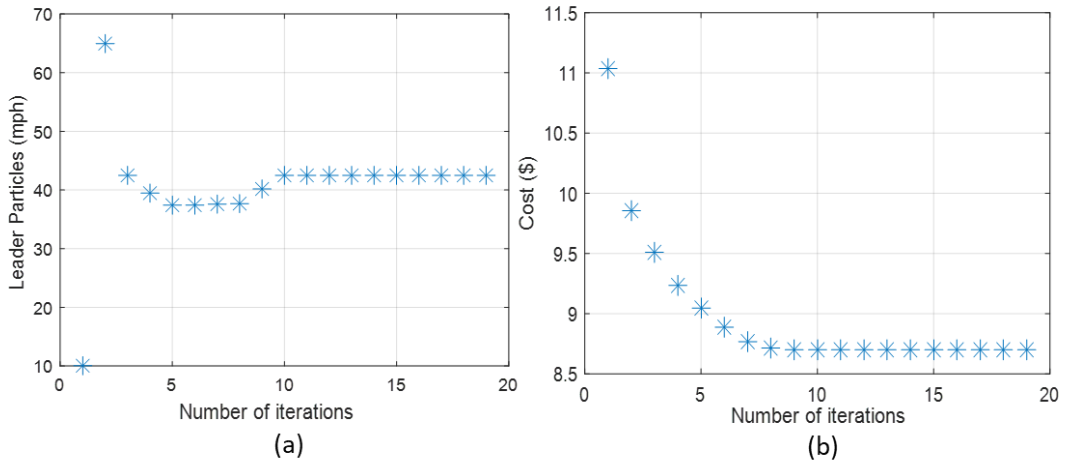

Figure 4.4: The global cost and the leaders of an interval as the iteration number increases. a) Leader particles b) Global cost.

4.3. Optimization Process

The optimization process is realized in two stages. The first stage includes energy consumption and battery degradation models; it simulates the EV with varying speeds to calculate energy consumption for a certain route. Route conditions and vehicle velocity are included in the simulation as inputs. Rolling resistance, aerodynamic drag, and gravitational forces are calculated based on route conditions. At a certain speed and torque, the efficiency of the motor drive system is determined via a look-up table. Therefore, the energy consumption is calculated. The output of the vehicle model is the energy consumption curves as a function of the vehicle speed for each route interval. The optimization stage generates the optimal energy driving cycle, charging power and time, based on the simulation, as shown in Fig. 4.5. Using penalty cost, driving phase cost, and charging phase cost as inputs, the optimization layer decides the charging power and time, and the speed profile of the vehicle to reduce the bus network overall cost.

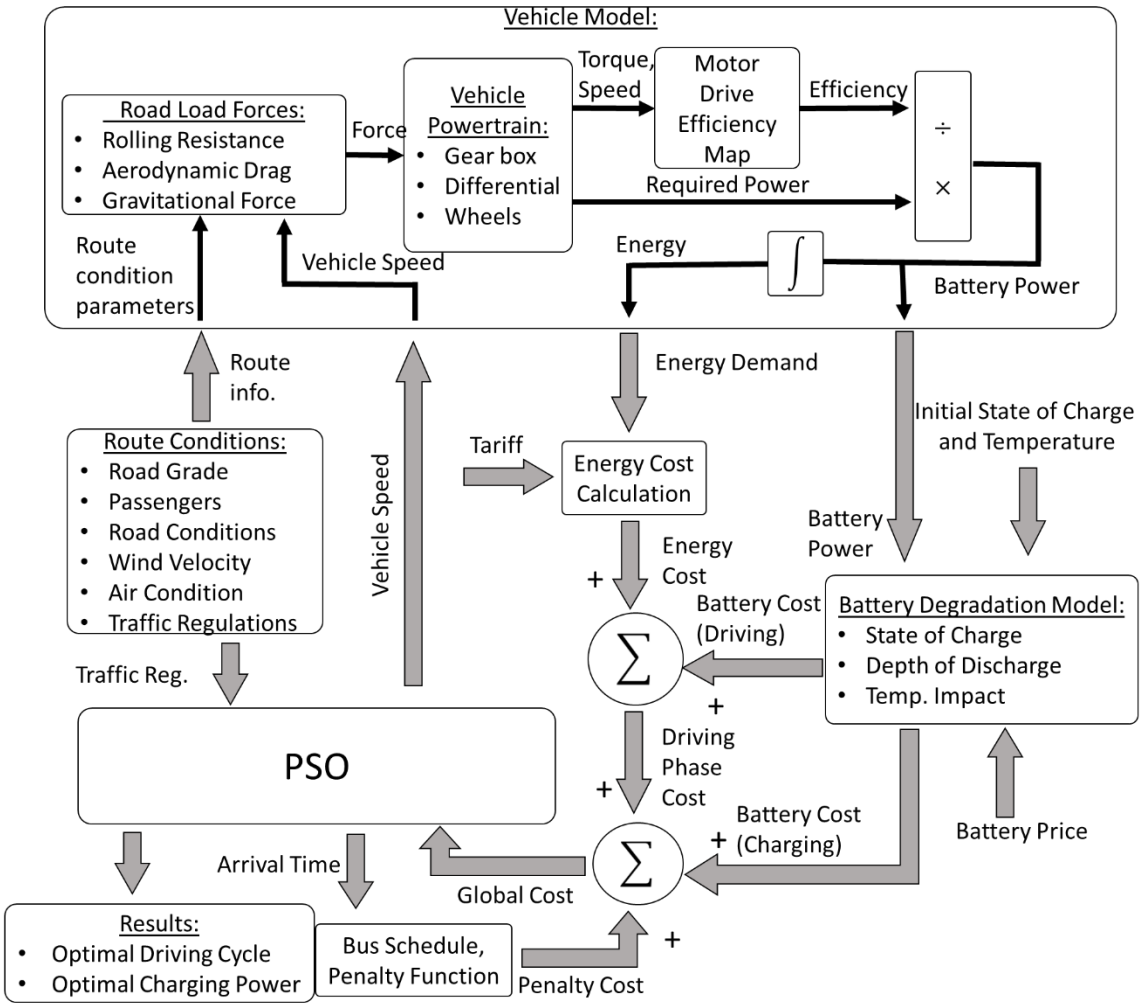

Figure 4.5: Block diagram of the optimization process.

4.4. Conclusions

This optimization chapter formulates the optimization problem using the models developed in Chapter III. The optimization problem was formulated using three different costs: the driving phase costs, the charging phase costs, and the penalty cost. Since the route is divided into 101 intervals; one hundred for the driving phase, and one for the charging phase, and since the penalty cost is added to the bus schedule, the optimization problem is formulated as a multi-objective optimization problem. Therefore, a PSO algorithm is applied for solving the problem. The algorithm is explained in detail, and the

overall optimization process is shown in block diagram form. The optimization results are shown, via case studies, in Chapter V.

CHAPTER V

CASE OPTIMIZATION AND SIMULATION RESULTS

In Chapters III and IV, the electric vehicle (Electric Vehicle) bus model is given, the “optimization problem” is defined, and a PSO algorithm is developed to solve the “optimization problem”. In this chapter, the optimization results are presented using case studies based on certain route scenarios that are specially prepared for demonstration purposes.

5.1. Case Studies

A selected number of case scenarios are prepared for demonstrating the impacts of different route conditions, as the impact magnitude of various route conditions varies. The optimized results are compared to un-optimized results to determine the cost savings that can be realized because of the proposed optimization. Like optimized results, un-optimized results also include driving cycle and charging times. Apart from acceleration and breaking, the un-optimized driving cycle is considered as a constant speed cycle, while the charging time is considered to be a round number, to ensure that the cycle is indeed un-optimized.

For demonstration purposes, multiple case scenarios are prepared so as to demonstrate varying route conditions.

5.1.1 Case Study I

The first case study is basic, and only investigates the impact of road grade and speed limits on speed profile.

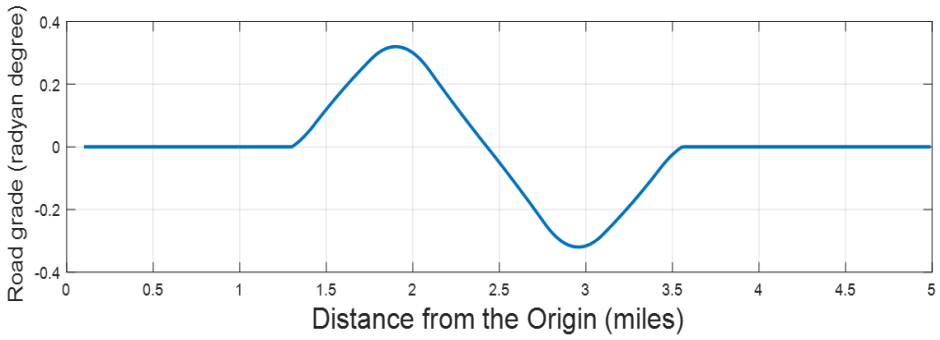

(a)

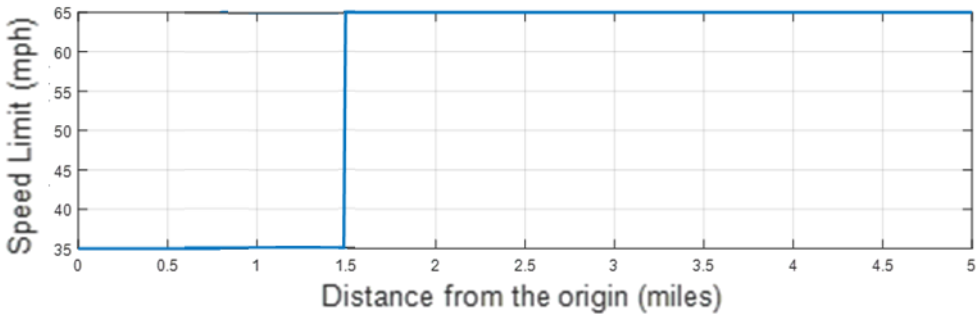

(b)

Figure 5.1: Route conditions of the case study 1. a) Road grade. b) Speed limit.

Figure 5.1 shows the route conditions of the first case study

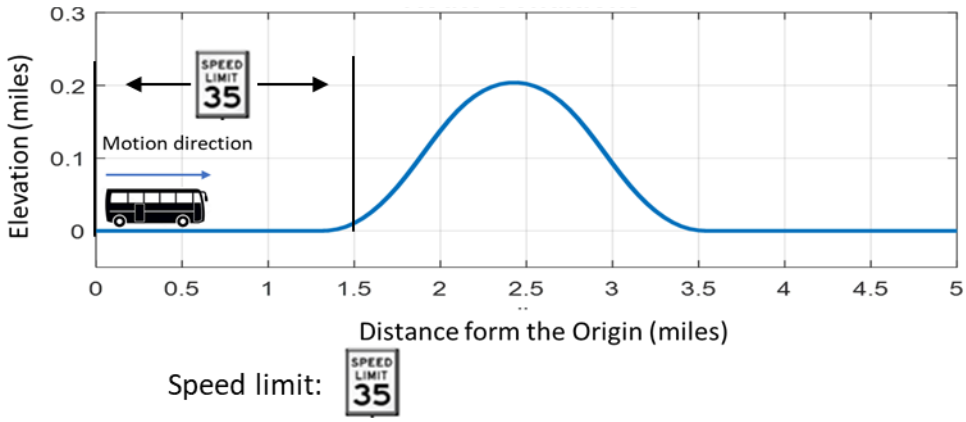

Figure 5.2: Visual representation of the bus route.

Visual route conditions of the case study are presented in Fig. 5.2.

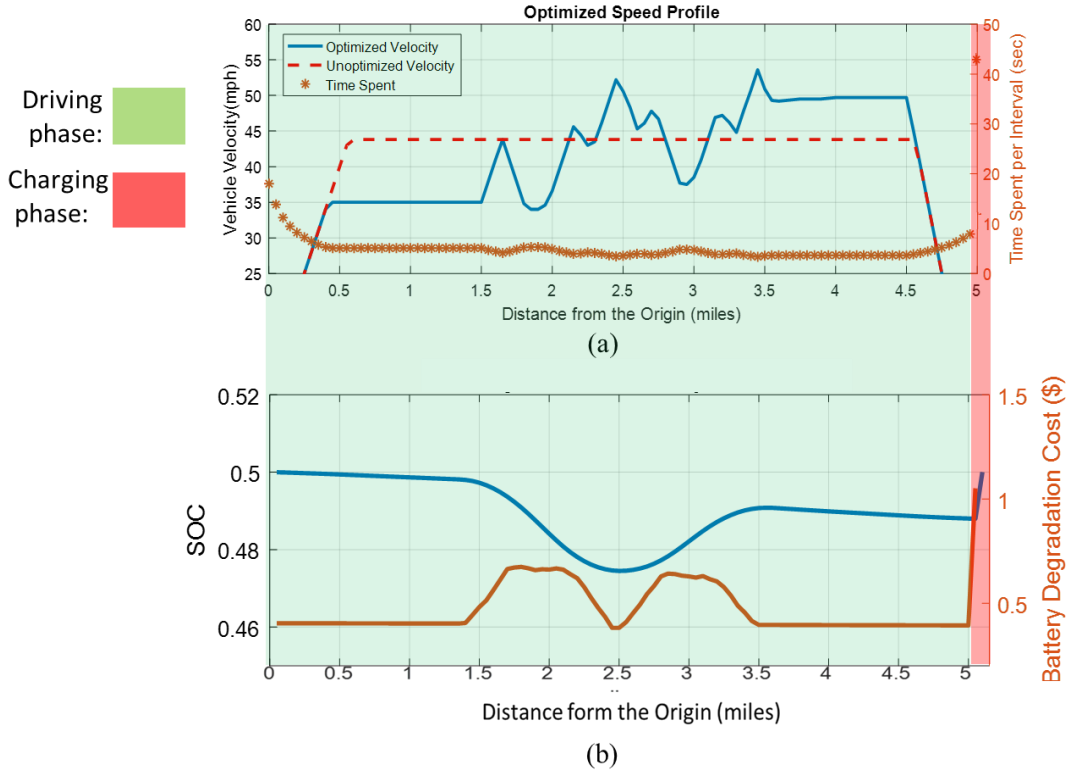

Figure 5.3: Optimized results for the first case study. a) Speed profile and time spent (driving and charging) on each interval of the route. b) Optimized battery SOC and cost.

Optimization results are presented in Fig. 5.3. Because the route segments (including charging at the bus stop) are divided into 100 intervals, the charging phase of the route is considered as the last interval where the vehicle speed is zero, and the battery power is negative because it is charging. At the bus stop, the battery of the vehicle gets charged up until its SOC reaches what it was at the previous bus stop.

Table 5.1: Optimization results for Case I.

Description	Optimized results	Un-optimized results	unit
Travel time	454.6	440	sec
Charging time	45.3	60	sec
Total time (Charging + traveling)	500	500	sec
Energy Consumption	2.05	2.24	kWh
Average speed	39.59	40.92	mph
Travel phase cost	56.2	58.04	$
Charging phase cost	1.1	1.03	$
Total cost (Charging + traveling)	57.3	59.07	$

5.1.2 Case Study II

This case study investigates the impact of road grade, speed limits, wind speed, and number of passenger.

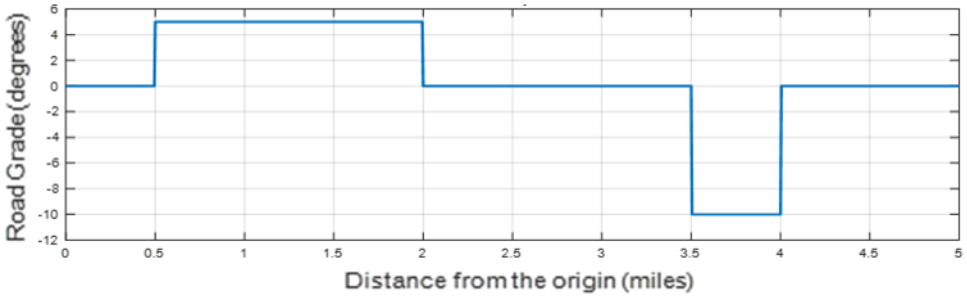

(a)

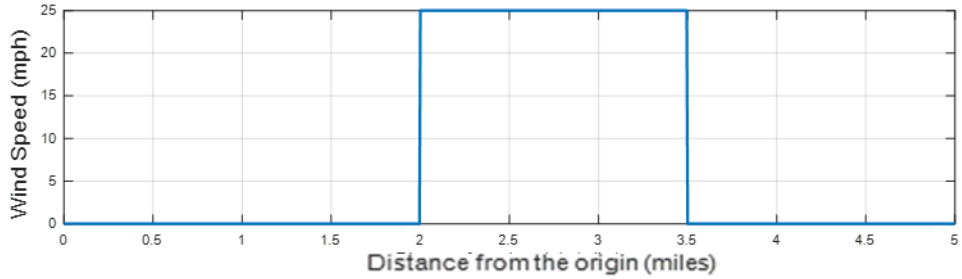

(b)

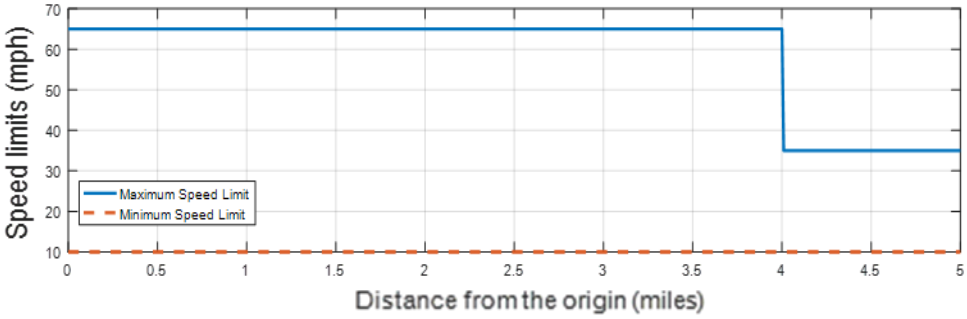

(c)

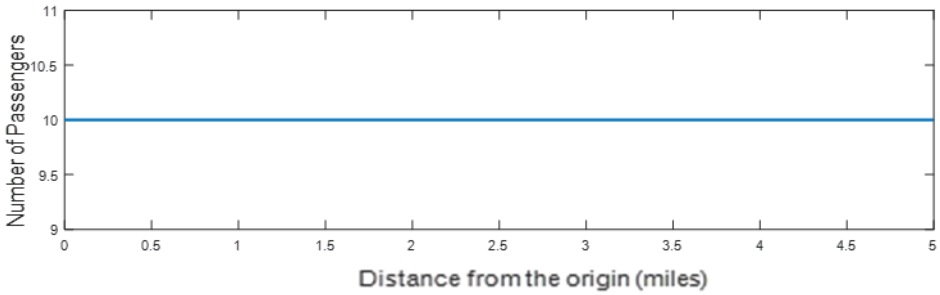

(d)

Figure 5.4: Route conditions for the case study. a) Speed limit. b) Road slope. c) Wind speed d) Passenger number.

Fig. 5.4 (a)-(d) present the speed limits, road slope, wind speed, and number of passengers throughout the route respectively.

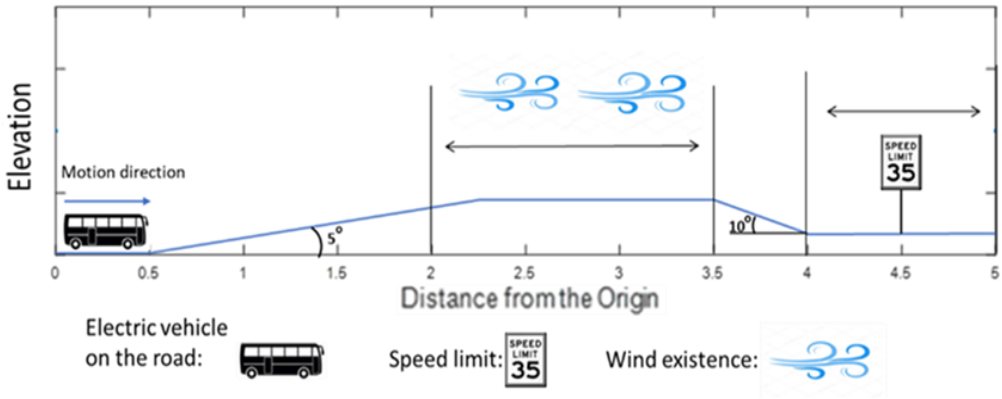

Figure 5.5: EV bus and its considered route condition for the case study.

A visual representation of the bus route is presented in Fig. 5.5.

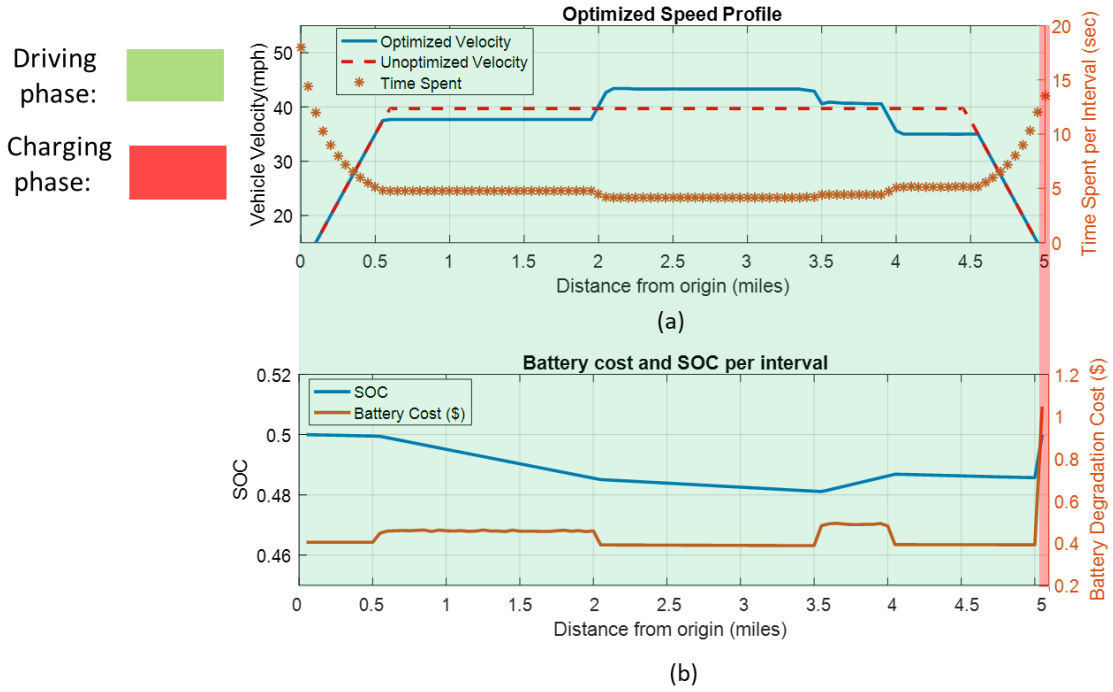

Figure 5.6: Optimized results for the second case study. a) Speed profile and time spent (driving and charging) on each interval of the route. b) Optimized battery SOC and cost.

The optimization results of this scenario, which were determined similarly to the ones from Case I, are presented in Fig. 5.6 and Table 5.2.

Table 5.2: Optimization results for Case II.

Description:	Optimized results	Un-optimized results	unit
Travel time	536	520	sec
Charging time	14	30	sec
Total time (Charging + traveling)	550	550	sec
Energy Consumption	0.76	0.91	kWh
Average speed	33.6	34.7	mph
Travel phase cost	43.76	45.6	$
Charging phase cost	1.1	.85	$
Total cost (Charging + traveling)	44.86	46.45	$

5.1.3 Case Study III

This case study investigates the impact of road grade, wind speed, and speed limits on the overall bus network cost.

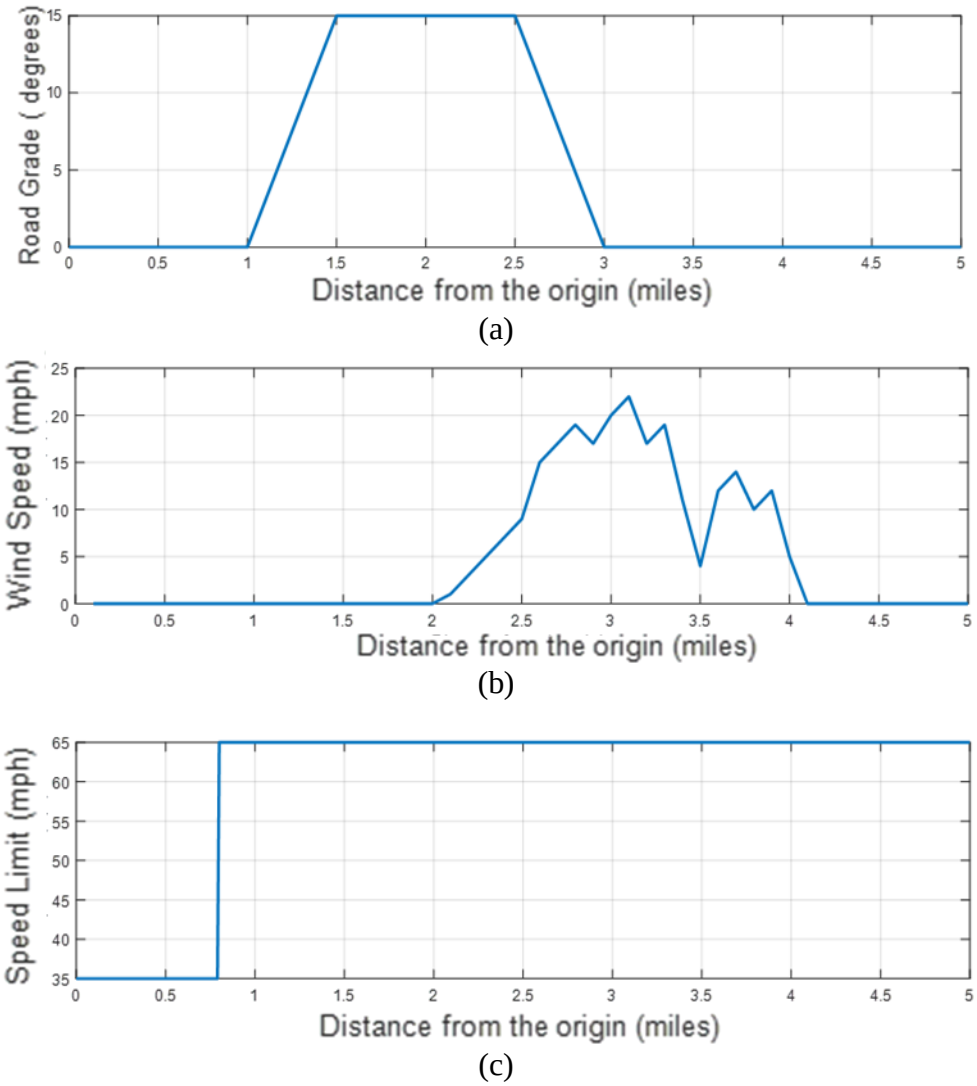

Figure 5.7: Route conditions for the case study. a) Road slope. b) Wind Speed. c) Speed limit.

Fig. 5.7 (a)-(c) presents the road grade, wind speed, and speed limits throughout the route respectively.

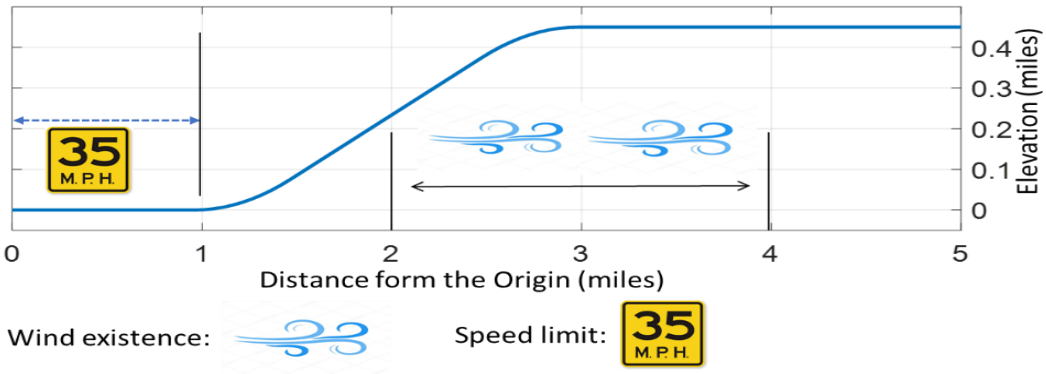

Figure 5.8: A visual representation of the bus route.

A visual representation of the bus route is illustrated in Fig. 5.8.

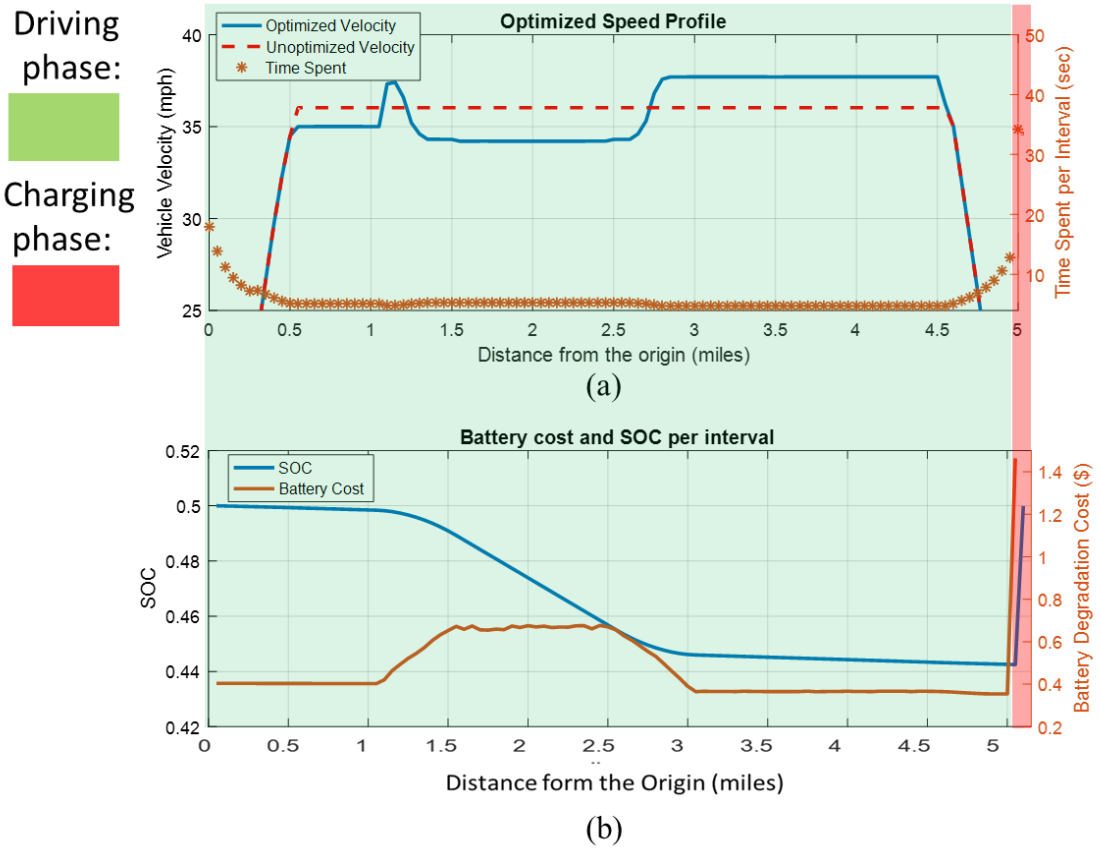

Figure 5.9: Optimized results for the third case study. a) Speed profile and time spent (driving and charging) on each interval of the route. b) Optimized battery SOC and cost.

The optimization results of this scenario are presented in Fig. 5.9. and Table 5.3.

Table 5.3: Optimization results for Case III.

Description:	Optimized results	Un-optimized results	unit
Travel time	545.95	520	sec
Charging time	34.05	60	sec
Total time (Charging + traveling)	580	580	sec
Energy Consumption	4.37	4.63	kWh
Average speed	32.9	34.6	mph
Travel phase cost	65.57	68.73	$
Charging phase cost	1.41	1.39	$
Total cost (Travel +charging)	66.98	70.12	$

5.2. Reduction of Battery Capacity

The three cases previously studied are considered to be parts of a theoretical bus network. To determine battery capacity reduction in the above case studies, let the bus network consist of four bus stops as shown in Fig. 5.10.

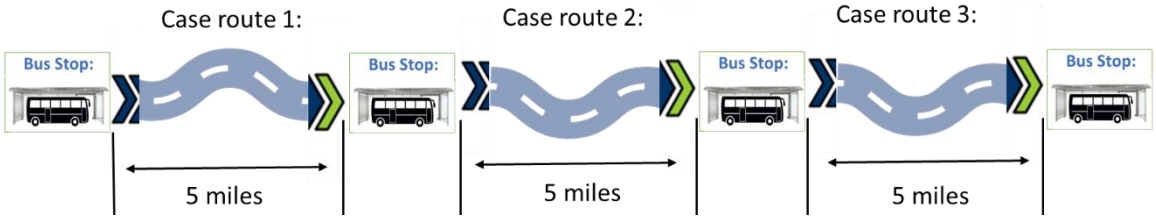

Figure 5.10: Considered bus route using previous case studies.

The required energy amounts have already been determined for the considered case studies. The case with the highest energy consumption is the Case III, as shown in Table 5.4. Since implementing the opportunity charging allows the vehicle to be charged at each

bus station, the minimum required battery capacity is considered to be the worst-case scenario, which is Case III. Thus, the required battery size for the considered bus network can be reduced from 7.15 to 4.37 kWh.

Table 5.4: Required minimum battery capacity for case studies.

	Case 1	Case 2	Case 3	Total
Required battery capacity (kWh)	2.02	0.76	4.37	7.15

5.3. Conclusions

As demonstrated in the case studies considered in this chapter, vehicle speed reacts dynamically depending upon road load forces, which are, in turn, ruled by the route conditions. The vehicle always follows the optimal speed of each interval of the route. The optimization algorithm also optimizes the charging time of the battery. The optimal charging time also changes based on route conditions. The optimization results indicate that the optimized charging phase cost is higher than that of the un-optimized charging phase cost, but the overall cost of the optimized bus network is lower than that of the un-optimized one. The overall running cost of the network is reduced from roughly 2% to 5%, depending on the case study and route conditions. Further, the required battery capacity is also reduced considering the case studies calculations.

CHAPTER VI

CONCLUSION AND FUTURE WORK

Recent developments in electric energy storage technology have allowed vehicle manufacturers to produce long-range and low-cost electric vehicles (EV) for common use. For many users, affordable EV technology has now become available. They are presently the first choice for inner-city transportation purposes. Thus, mainstream adoption of EVs is becoming more imminent each year. As environmentally-friendly transportation solutions are wide spreading, fossil fuels, which have a harmful effect on the atmosphere, are encouraging city administrators to replace conventional buses with less harmful transportation methods. As a result, EV technology is also expected to be adopted by big city administrations as their new public transportation means. However, the relatively high cost of energy storage technology (Li-ion batteries) is still a major problem that needs to be tackled. Although Li-ion batteries can store much higher levels of energy, with higher power levels, compared to other alternatives, they are significantly heavy and require a significant amount of vehicle space, which negatively impacts the energy consumption of EVs.

This study aims to reduce the costly battery size and energy consumption of an EV based city bus network. Two methods are introduced to resolve the two major issues mentioned above for the near future EV-bus networks.

First, several bus charging patterns such as ‘overnight charging’, ‘battery swap’, and ‘opportunity charging’, are investigated in the literature to lower EV bus battery capacity requirements. Among these, the ‘opportunity charging’ pattern is chosen because it reduces the required battery capacity. Although ‘opportunity charging’ means charging the batteries at each bus stop, which impacts the battery storage lifespan, this impact is reduced by including the battery degradation cost as an additional constraint in the optimization problem. For battery lifespan estimation, a battery degradation model that includes three parameters: state of charge (SOC), depth of discharge (DOD), and temperature impact, is used.

To reduce the electricity consumption, an electrically-operated bus model is developed. The model is used to estimate the energy consumption of the vehicle. Further, the impact of the route conditions (road grade, passenger quantity, wind speed, speed limits, traffic regulations) on energy consumption is modeled. The magnitude of the impact of the route conditions is governed by three types of forces: aerodynamic drag, rolling resistance, and gravitational force. Therefore, the tractive force has to overcome these forces to move the vehicle forward. Efficiency maps of the electric engine and the inverter are acquired and used in the electric bus model. Thus, energy consumption curves of each segment of the route on different route conditions and vehicle speed are created and used as constraints in the optimization problem. Another constraint that the optimization problem includes is a penalty function. Since most optimal speed profiles might conflict with the bus schedule, the defined penalty constraint increases the global cost of the optimized system when conflicts occur. Therefore, it ensures that the bus reaches the next bus stop on time while optimizing the speed profile and battery charging period

simultaneously. Eventually, a multi-objective optimization problem that considers all of the mentioned constraints is defined, and an optimization algorithm is developed.

An optimization algorithm required for determining the optimal speed profile of the route and the charging time and power at the bus stop while considering the constraints. Thus, a particle swarm optimization algorithm is developed in MATLAB. Using the simulation results, the optimization algorithm generates the optimal speed profile, energy consumption and charging time while considering battery degradation and bus schedule.

Optimization results are demonstrated via multiple case studies and compared to the un-optimized case studies in Chapter IV. A comparison of the optimized and un-optimized results reveal that optimized results save a significant amount of energy cost. While the magnitudes of some route conditions such as road grade, passenger quantity, and wind speed increase the saved energy percentage, others such as speed limits and traffic slow-downs decrease it because of being limiting factors on the speed profile.

This study proposes the opportunity charging, along with the battery degradation model, as a solution to the costly battery needs of electrically operated city bus networksto reduce battery cost as well. Furthermore, it proves that a considerable amount of energy can be saved if the speed profile of an EV-based bus network is optimized considering route conditions, and a penalty function is introduced in the optimization problem so that the bus schedule is not compromised. However, efficiency maps of the electric engine and the inverter are used for energy consumption calculations which might fade over time. This situation requires that the data used in the EV model be updated. As for future work, a sensor system can be developed to keep track of the efficiency of the components and

update the data in the model as the bus is running on duty without requiring additional efficiency tests.

REFERENCES:

[1] C. Vyas, D. Hurst, and J. Gartner, “Electric vehicle consumer survey,” Pike Research, Tech. Rep., 2011.

[2] Mehrdad Ehsani, Yimin Gao, Sebastien E. Gay, and Ali Emadi, Modern Electric, Hybrid Electric, and Fuel Cell Vehicles: Fundamentals, Theory, and Design.: CRC Press, 2004.

[3] M. Kuriyama, S. Yamamoto and M. Miyatake, "Theoretical study on Eco-Driving Technique for an Electric Vehicle with Dynamic Programming," *2010 International Conference on Electrical Machines and Systems*, Incheon, 2010, pp. 2026-2030.

[4] Weimin Li, Guoqing Xu, Zhancheng Wang and Yangsheng Xu, "Dynamic energy management for hybrid electric vehicle based on adaptive dynamic programming," *2008 IEEE International Conference on Industrial Technology*, Chengdu, 2008, pp. 1-6.

[5] W. Feng and M. Figliozzi, "An economic and technological analysis of the key factors affecting the competitiveness of electric commercial vehicles: A case study from the USA market," Transportation Research Part C: Emerging Technologies, vol. 26, pp. 135–145, Jan. 2013.

[6] J. Randolph and G. Masters, Energy for Sustainability: Technology, Planning, Policy. Island Press, 2008.

[7] N.-O. Nylund, K. Koponen, “Fuel and Technology Alternatives for Buses - Overall Energy Efficiency and Emission Performance”, VTT Technology 46,ISBN978-951-38-7869-6, http://www.vtt.fi/inf/pdf/technology/2012/T46.pdf (website accessed 31.10.2017)

[8] N. A. El-Taweel, M. Mohamed and H. E. Farag, "Optimal design of charging stations for electrified transit networks," 2017 IEEE Transportation Electrification Conference and Expo (ITEC), Chicago, IL, 2017, pp. 786-791.

[9] S. Bashash, S.J. Moura, J.C. Forman, and H.K. Fathy, “Plug-In Hybrid Electric Vehicle Charge Pattern Optimization for Energy Cost And Battery Longevity,” Journal of Power Sources, vol. 196, pp, 541-549, Jul. 2010.

[10] “Mind the gap: London's buses embrace wireless charging,” BBC, 2014. [Online]. Available at: http://www.bbc.com/future/story/20141028-the-bus-that-recharges-on-the-go. [Accessed: Jul-2017].

[11] J. Y. Wong, Theory of Ground Vehicles. New York: Wiley-Interscience, 2001

[12] I. Husain, Electric and Hybrid Vehicles: Design Fundamentals, 2nd edition. CRC Press, 2010.

[13] R. Abousleiman and O. Rawashdeh, "Energy consumption model of an electric vehicle," 2015 IEEE Transportation Electrification Conference and Expo (ITEC), Dearborn, MI, 2015, pp. 1-5.

[14] Y. Zhang, W. Wang, Y. Kobayashi and K. Shirai, "Remaining driving range estimation of electric vehicle," 2012 IEEE International Electric Vehicle Conference, Greenville, SC, 2012, pp. 1-7.

[15] P. D. Blair, "Modeling energy and power requirements of electric vehicles," Energy Conversion, vol. 18, no. 3, pp. 127{134, 1978.

[16] J. J. Valera, B. Heriz, G. Lux, J. Caus and B. Bader, "Driving cycle and road grade on-board predictions for the optimal energy management in EV-PHEVs," 2013 World Electric Vehicle Symposium and Exhibition (EVS27), Barcelona, 2013, pp. 1-10.

[17] Q. Yan, B. Zhang and M. Kezunovic, "Optimization of electric vehicle movement for efficient energy consumption," 2014 North American Power Symposium (NAPS), Pullman, WA, 2014, pp. 1-6.

[18] F. Badin et al., "Evaluation of EVs energy consumption influencing factors, driving conditions, auxiliaries use, driver's aggressiveness," 2013 World Electric Vehicle Symposium and Exhibition (EVS27), Barcelona, 2013, pp. 1-12.

[19] H. A. Jed, A. Mieze, R. Simon and J. M. Vinassa, "An electric vehicle model and a driving cycle for mail delivery use," Proceedings of the 2011 14th European Conference on Power Electronics and Applications, Birmingham, 2011, pp. 1-8.

[20] M. Karamuk, "A survey on electric vehicle powertrain systems," International Aegean Conference on Electrical Machines and Power Electronics and Electromotion, Joint Conference, Istanbul, 2011, pp. 315-324.

[21] D. G. Dorrell, A. M. Knight, M. Popescu, L. Evans and D. A. Staton, "Comparison of different motor design drives for hybrid electric vehicles," 2010 IEEE Energy Conversion Congress and Exposition, Atlanta, GA, 2010, pp. 3352-3359.

[22] D. Bucherl, R. Nuscheler, W. Meyer and H. G. Herzog, "Comparison of electrical machine types in hybrid drive trains: Induction machine vs. permanent magnet synchronous machine," 2008 18th International Conference on Electrical Machines, Vilamoura, 2008, pp. 1-6.

[23] T. Finken, M. Felden and K. Hameyer, "Comparison and design of different electrical machine types regarding their applicability in hybrid electrical vehicles," 2008 18th International Conference on Electrical Machines, Vilamoura, 2008, pp. 1-5.

[24] A. Hoke, A. Brissette, K. Smith, A. Pratt and D. Maksimovic, "Accounting for Lithium-Ion Battery Degradation in Electric Vehicle Charging Optimization,"in IEEE Journal of Emerging and Selected Topics in Power Electronics, vol. 2, no. 3, pp. 691-700, Sept. 2014.

[25] M. Koller, T. Borsche, A. Ulbig and G. Andersson, "Defining a degradation cost function for optimal control of a battery energy storage system," 2013 IEEE Grenoble Conference, Grenoble, 2013, pp. 1-6.

[26] S. Han, and H. Aki, "A Practical Battery Wear Model for Electric Vehicle Charging Applications," Appl. Energy, vol. 113, pp. 1100–1108, Jan. 2014.

[27] F. Baronti et al., "Implementation of the fast charging concept for electric local public transport: The case-study of a minibus," in 2015 IEEE 13th International Conference on Industrial Informatics (INDIN), 2015, pp. 1284–1289.

[28] G. Fabbri et al., "An innovative system for a clean and sustainable public transport system in smart cities," 2016 IEEE 25th International Symposium on Industrial Electronics (ISIE), Santa Clara, CA, 2016, pp. 974-979.

[29] N. A. El-Taweel, M. Mohamed and H. E. Farag, "Optimal design of charging stations for electrified transit networks," 2017 IEEE Transportation Electrification Conference and Expo (ITEC), Chicago, IL, 2017, pp. 786-791.

[30] M. Mohamed, H. Farag, N. El-Taweel, M. Ferguson, "Simulation of electric buses on a full transit network: Operational feasibility and grid impact analysis", Electric Power Systems Research, vol. 142, pp. 163175, Jan. 2017. 35

[31] A. O. Al-Jazaeri, L. Samaranayake, S. Longo and D. J. Auger, "Fuzzy Logic Control for energy saving in Autonomous Electric Vehicles," 2014 IEEE International Electric Vehicle Conference (IEVC), Florence, 2014, pp. 1-6.

[32] H. Ko, T. Koseki and M. Miyatake" Application of Dynamic Programming to Optimal Running Profile of Train" COMPRAIL 2004, Dresden, 2004.

[33] M. Karmakar and A. K. Nandi, "Trip planning for electric vehicle through optimal driving using genetic algorithm," 2016 IEEE 1st International Conference on Power Electronics, Intelligent Control and Energy Systems (ICPEICES), Delhi, 2016, pp. 1-6.

[34] KE Parsopoulos, MN Vrahatis, "Particle swarm optimization method in multiobjective problems", Proceedings of the ACM 2002 symposium on applied computing (SAC'2002), pp. 603-607.

[35] H. Ling, X. Zhou, Y. Xiao and X. Jiang, "An improved PSO algorithm for constrained multiobjective optimization problems," 2011 International

Conference on Computer Science and Service System (CSSS), Nanjing, 2011, pp. 3859-3863.

[36] J Moore and R Chapman, “Application of particle swarm to multiobjective optimization”, Department of Computer Science and Software Engineering, Auburn University, 1999.

[37] M. Grossard, S. Kachroudi and N. Abroug, "An optimal energy-based approach for driving guidance of full Electric Vehicles," 2012 IEEE International Symposium on Industrial Electronics, Hangzhou, 2012, pp. 1708-1713.

[38] E. Kim, J. Lee and K. G. Shin, "Real-time prediction of battery power requirements for electric vehicles," 2013 ACM/IEEE International Conference on Cyber-Physical Systems (ICCPS), Philadelphia, PA, 2013, pp. 11-20.

[39] R. Lot and S. A. Evangelou, "Green driving optimization of a series hybrid electric vehicle," 52nd IEEE Conference on Decision and Control, Firenze, 2013, pp. 2200-2207.26

[40] W. Li, G. Xu, Z. Wang and Y. Xu, "Dynamic energy management for hybrid electric vehicle based on adaptive dynamic programming," 2008 IEEE International Conference on Industrial Technology, Chengdu, 2008, pp. 1-6.27

[41] I. Kolmanovsky, I. Siverguina, B. Lygoe, ”Optimization of Powertrain Operation Policy for Feasibility Assessment and Calibration: Stochastic Dynamic Programming Approach,” presented at American Control Conference, Anchorage, Alaska, 2002.28

[42] M. Kuriyama, S. Yamamoto and M. Miyatake, "Theoretical study on Eco-Driving Technique for an Electric Vehicle with Dynamic Programming," 2010 International Conference on Electrical Machines and Systems, Incheon, 2010, pp. 2026-2030.

APPENDIX A: ELECTRIC VEHICLE SIMULATION

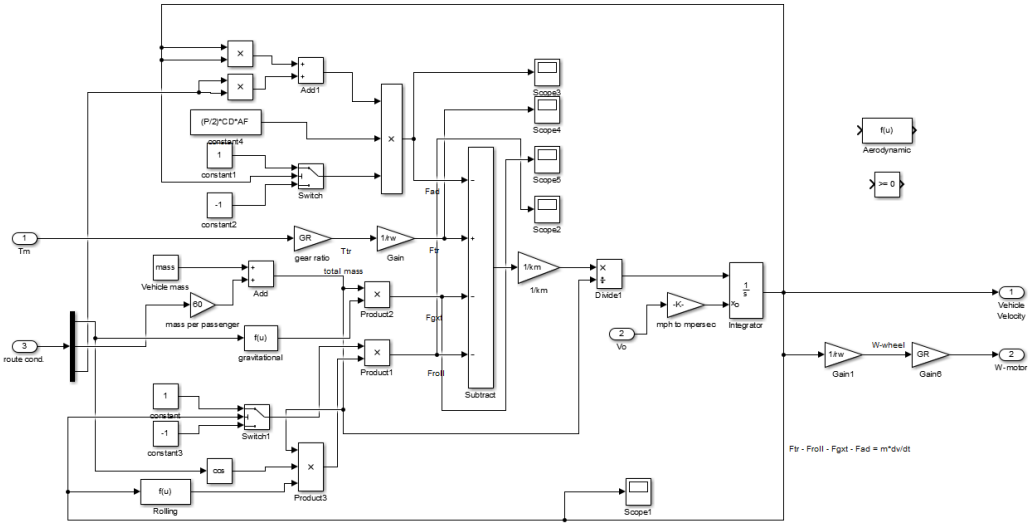

A.1.: Simulink simulation of the EV physical dynamics.

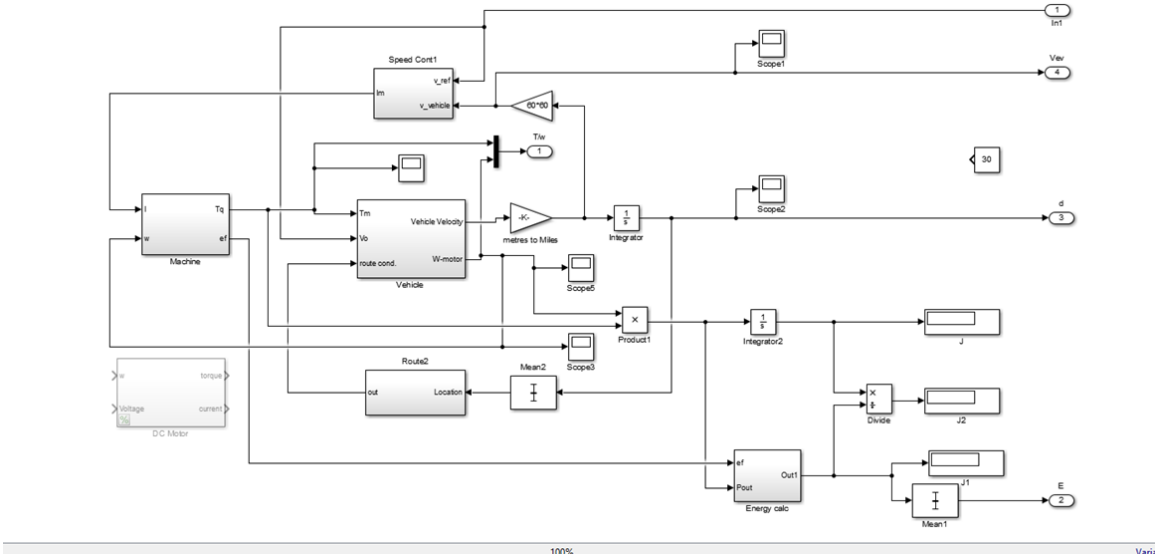

A.2.: EV Simulink simulation.

```
clearvars -except E E1
close all
numinterval=100;
int_speed=10;
top_speed=65;
speedincrement=2500;
increment=.1;
maxx=55001;
minn=1;
t=600;
tmax=660;
inspeed=15000;
numparticle=1000;
SOCo=.5;
SOC(1)=SOCo;
GT=.3;
mass=1400;
rw=.3;
GR=8;

%speedmax=[35,35,35,35,35,35,35,35,35,35,35,35,35,35,35,35,35,
35,35,35,35,35,                35,35,35,35,35,35,35,35,35,35,
65,65,65,65,65,65,65,65,65,65,65,65,65,65,65,65,65,65,65,65
,65,65,65,65,65,65,65,65,65,65,65,65,65,65,65,65,65,65,65,6
5,65,65,65,65,65,65,65,65,65,65,65,65,65,65,65,65,65,65,65,
50,40,35,30,25,20,15,13,11,10];
%speedmax=interp(speedmax,numinterval);
speedmax=[65,65,65,65,65,65,65,65,65,65,65,65,65,65,65,65,6
5,65,65,65,65,                                              65
,65,65,65,65,65,65,65,65,65,65,65,65,65,65,65,65,65,65,65,6
5,65,65,65,65,65,65,65,65,65,65,65,65,65,65,65,65,65,65,65,
65,65,65,65,65,65,65,65,65,65,65,65,65,65,65,65,65,65,65,65
,65,65,65,65,65,60,55,50,45,40,35,30,25,20,15,10,10,10,10];

speedmax=round((speedmax-9.9999)*maxx/55)+1;
speedmin=[ 10 10 10 10 10 10 10 10 10 10];
speedmin=interp(speedmin,numinterval);
%
[intervalcosts,intervaltimes]=evaluate(E1,numinterval,int_s
peed,top_speed,increment);
[intervalcostst,intervaltimest]=interp_opt(intervalcosts,
intervaltimes,numinterval );

%[intervalcosts,intervaltimes]=evaluate(E1,numinterval,int_
speed,top_speed,increment);
```

```
[torquematrix,omegamatrix]=eval_torque_omega(E1(:,5),E1(:,6
));
[torquematrix_t,omegamatrix_t]=interp_opt(torquematrix,omeg
amatrix,numinterval);

% intervalcosts(:,5)=-.0001*data;
timingcostf = @(x) 100.*abs(x.^2);

%assign initial speeds

intmin(1:numinterval,1)=minn;
intmax(1:numinterval,1)=maxx;




for int=1:numinterval

%     r = randi([intmin(int),intmax(int)],numparticle,1);
      r=1000;
    randomcosts(int,:) =   intervalcoststst(r,int);
    randomtimes(int,:) =   intervaltimest(r,int);
    randomspeeds(int,:)=   r;

    [leader_costs(int,:),   lider_index(int,:)]            =
min(randomcosts(int,:));
    leader_times(int,:) = randomtimes(lider_index(int,:));
    leader_speeds(int,:)=randomspeeds(lider_index(int,:));

    travelcost = sum(leader_costs);
    traveltime = sum(leader_times);
    timingpenalty=timingcostf(t-traveltime);
    totalcost(1)=travelcost+timingpenalty;
    ttcost(1)=min(totalcost);
end


for i=2:20


    for int=1:numinterval

%         if tolerancematrix(int,i)==1;
%             break;
%         end
%
```

```
%             intmin(1:numinterval,1:100)=1;
%             intmax(1:numinterval,1:100)=55001;


        for j=1:1

            r                                                    =
randi([intmin(int,j),intmax(int,j)],numparticle,1);

            if  2<=int
                for k=1:numparticle
                    if   r(k)   -   leader_speeds(i,int-1)<-
speedincrement;
                        r(k)=leader_speeds(i,int-1)-
speedincrement;
                    end

                    if    r(k)    -    leader_speeds(i,int-
1)>speedincrement;
                        r(k)=leader_speeds(i,int-
1)+speedincrement;
                    end
                end
            else
                r(1:numparticle)=1;
            end



            randomcosts_int =   intervalcostst(r,int);
            randomtimes_int =   intervaltimest(r,int);
            randomspeed_int =   r;


            for k=1:numparticle

                 leader_costs(int)     =  randomcosts_int(k);
                 leader_times(int)     =  randomtimes_int(k);
                 leader_speeds(int)    =  randomspeed_int(k);

                [bcost(int),SOC(int+1)]=
batterycost(randomcosts_int(k),randomtimes_int(k),SOC(int))
;


                 travelcost(k,:)                             =
sum(leader_costs)+bcost(int);
```

```
                traveltime(k,:)      =  sum(leader_times);

            end

            timingpenalty=timingcostf(t-traveltime);
            [bcost_charging(i),
SOC_charging]=batterycost(travelcost.*(-1), tmax-traveltime,
SOC(end));

totalcost=(travelcost+timingpenalty)*GT+bcost_charging(i);

            [value(j), indexx(j)]=best(totalcost);

            leader_costs(int) =randomcosts_int(indexx(j));
            leader_times(int) =randomtimes_int(indexx(j));

leader_speeds(i,int)=randomspeed_int(indexx(j));


            SOC_c(i)=SOC_charging(indexx(j));
            t_charging(i)=tmax-sum(leader_times);
            toff(i)=t-sum(leader_times);


            range=300+30000-i*1000;
            range(range<500)=1000;

            rng(i)=range;
            intmin(int,j)= round(randomspeed_int(indexx(j))-
range);
            intmax(int,j)=
round(randomspeed_int(indexx(j))+range);


%             if intmin(int+1,j+1)-intmin(int,j+1)>455
%                 intmin(int+1,j+1)=intmin(int,j+1)+455;
%             end
%             if intmin(int+1,j+1)-intmin(int,j+1)<-455
%                 intmin(int+1,j+1)=intmin(int,j+1)-455;
%             end
%
            % if- else block speed limits here

            if                      intmin(int)<speedmin(int)
intmin(int)=speedmin(int); end
%             intmin(intmin<speedmin(int)) = speedmin(int);
```

```
            if                      intmin(int)>speedmax(int)
intmin(int)=speedmax(int); end
%             intmin(intmin>speedmax(int)) = speedmax(int);
            if                      intmax(int)>speedmax(int)
intmax(int)=speedmax(int); end
%             intmax(intmax>speedmax(int)) = speedmax(int);
            if     intmax(int)<speedmin(int)     intmax(int)=
speedmax(int); end
%             intmax(intmax<speedmin(int)) = speedmin(int);

        end

    end

     ttcost(:,i)=sum(leader_costs);
     ttspeeds(:,i)=leader_speeds(i,:);


%     for k=1:numinterval
%
%            if    abs( (leader_speeds(i,k)-leader_speeds(i-
1,k))*55/55001+10 )<= 5
%
%             tolerancematrix(i,k)=1;
%
%         end
%     end


     [globalmin(i-1), globalindex(i-1)]=min(ttcost);
end

torque_index=ttspeeds(:,globalindex(end));
for l=1:100
    tt_torque(l)=torquematrix_t(torque_index(l),l);
    tt_omega(l)=omegamatrix_t(torque_index(l),l);
end
tt_torque(100)=tt_torque(99);
tt_omega(1)=tt_omega(2);
tt_omega_rpm=tt_omega*30/pi;

%plotting
ttspeeds_miles=ttspeeds*55/55001+10;
ttspeeds_miles=ttspeeds_miles(:,globalindex(end));
ttspeeds_miles=[ttspeeds_miles; 0];
ttspeeds_miles(1)=0;
```

```
ttspeeds_mps=ttspeeds_miles.*0.447;
ttspeeds_mps(101)=0;

for i=1:100
tt_acc(i)= ttspeeds_mps(i+1)-ttspeeds_mps(i);
end
torque_m=tt_acc.*mass*rw/GR+tt_torque;

ttspeeds(:,globalindex(end))*55/55001+10;
tttimes=
60*60*0.05./(ttspeeds(:,globalindex(end))*55/55001+10);
tttimes=[tttimes; t_charging(globalindex(end))]/60;
tttimes(1)=.3;


globalmin(end)
i
globalindex(end)
x_axis=0:0.05:5;
figure(111)
p(1)=plot(x_axis,ttspeeds_miles);
p(1).LineWidth = 2;
title('Optimized Speed Profile')
xlabel('Intervals')
ylabel('Vehicle Velocity(mph)')
axis([0 5 10 45 ])
yyaxis right
p(2)=plot(x_axis,tttimes*60,'*');
p(2).LineWidth = 1;
grid
ylabel('Time Spent per Interval (sec)')



figure(112)
p(1)=plot([SOC SOC_c(globalindex(end))]);
p(1).LineWidth = 2;
title('Battery cost and SOC per interval')
xlabel('Intervals')
ylabel('SOC')
axis([0 103 .45 .52 ])
hold on
yyaxis right
p(2)=plot([bcost bcost_charging(globalindex(end))]);
p(2).LineWidth = 2;
ylabel('Battery Degradation Cost ($)')
grid
```

```
axis([0 103 .2 1 ])



figure(113)
p(1)=plot(tt_torque,'c');
p(1).LineWidth = 2;
title('Torque Profile')
xlabel('Intervals')
ylabel('Torque(Nm)')
hold on
p(2)=plot(torque_m,'--');
p(2).LineWidth = 2;
p(2).Color='b';


yyaxis right
p(3)=plot(tt_omega_rpm,'*');
p(3).Color = 'r';
p(3).LineWidth = 1;
grid
axis([0 100 2000 5000 ])
ylabel('Angular Velocity (RPM)')
legend('Load torque','Machine Torque','Ang. Velocity')


function [Cbattery, SOC]= batterycost (E,topr,SOCo)
% %battery degradation cost fucntion
%battery degration effect of each interval
%  E=[5000 1000];
%  topr=[10 4];
%  SOCo=0.5;
%////////////////////
Q=75;
tch=1;
Yhr=1760;
Cbat=40000;
m=30;
Qf=Q*0.7;
n=15;
d=1;
Rth=2e-4;
Tamb=25; % ambient battery temperature in Celc
CO=0.15;
a=2;
b=40;
m=30;
```

```
sz=size(E);
Pbattery=E./topr;
Bcap=1000; %kWh
% temperature effect
T=Tamb+Rth*abs(Pbattery);
% L=a*Q*exp(b*Q./T);
L=a*exp(b./T);
Ct=Cbat*(1./(Yhr*L))*CO;

%SOC effect
SOC=SOCo-E/Q/Bcap/60/60;
%SOC=SOCo+Pbattery*topr;
SOCa=(SOCo+SOC)/2;
Csoc=Cbat*((m.*SOCa-d)/(Qf*n*Yhr));

%DOD effect
DOD=abs(SOC-SOCo);
Cdod=(((-0.84376.*(DOD).^5)+(2.281.*(DOD).^4)+(-
2.2257.*(DOD).^3)+(1.1142.*(DOD).^2)+(-
0.385.*(DOD))+0.15923));

%total battery cost
    for k=1:sz(2)
        Cbattery(k)=max([Csoc(k) Ct(k) Cdod(k)]);
    end

end



   function                                                    [y1,
y2]=evaluate(E1,numinterval,int_speed,top_speed,increment)
% % % % function evaluate

%  top_speed=65;
%  int_speed=10;
%  increment=.1;
%  numinterval=10;

simout=round(E1,5);
clear intervalcosts
sizeofdata=55100;


  intervalcosts(:,1)=simout(1:sizeofdata,1);

  intervalcosts=reshape(intervalcosts,[numinterval,551])';
```

```
  for i=1:551
      for j=2:numinterval
          intervalcostsfin(i,j)=intervalcosts(i,j)-
intervalcosts(i,j-1);
      end
  end
costmatrix(:,1)=1*intervalcosts(:,1);
costmatrix(:,2:numinterval)=1*intervalcostsfin(:,2:numinter
val);

%time evaluation
for i=2:551*numinterval+1
    int_time(i-1,1)=simout(i,4)-simout(i-1,4);
end

timematrix=reshape(int_time,[numinterval, 551])';


 y1=costmatrix;
 y2=timematrix;
end

function
[intervalcostst,intervaltimest]=interp_opt(intervalcosts,
intervaltimes,numinterval )

% numinterval=100;
% int_speed=10;
% top_speed=65;
% increment=.1;
%[intervalcosts,intervaltimes]=evaluate(E1,numinterval,int_
speed,top_speed,increment);

for i=1:numinterval

    v = intervalcosts(:,i);
    x=10:.1:65;
    xq = 10:.001:65;
    vq1 = interp1(x,v,xq);

%     plot(xq,vq1)
    costmatrix(:,i)=vq1;

end
intervalcostst=costmatrix;
```

```
for i=1:numinterval

    v = intervaltimes(:,i);
    x=10:.1:65;
    xq = 10:.001:65;
    vq1 = interp1(x,v,xq);


    timematrix(:,i)=vq1;

end
intervaltimest=timematrix;
end



function
[torquematrix,omegamatrix]=eval_torque_omega(torque,omega)

% simout=E1;
% torque=simout(:,5);
% omega=simout(:,6);

torque=torque(1:55100);
omega=omega(1:55100);


torquematrix=reshape(torque,[100,551])';
omegamatrix=reshape(omega,[100,551])';

end
```